Bioengineering Thymus Organoids to Restore Thymic Function and Induce Donor-Specific Immune Tolerance to Allografts

Yong Fan[1], Asako Tajima[1], Saik Kia Goh[2], Xuehui Geng[3], Giulio Gualtierotti[3], Maria Grupillo[3], Antonina Coppola[3,4], Suzanne Bertera[1], William A Rudert[1], Ipsita Banerjee[2], Rita Bottino[1] and Massimo Trucco[1]

[1]Institute of Cellular Therapeutics, Allegheny Health Network, Pittsburgh, Pennsylvania, USA; [2]Department of Chemical and Petroleum Engineering, University of Pittsburgh School of Engineering, Pittsburgh, Pennsylvania, USA; [3]Division of Immunogenetics, Department of Pediatrics, University of Pittsburgh School of Medicine, Pittsburgh, Pennsylvania, USA; [4]Current address: Section of Endocrinology, Dipartimento Biomedico di Medicina Interna e Specialistica (DIBIMIS), University of Palermo, Palermo, Italy

One of the major obstacles in organ transplantation is to establish immune tolerance of allografts. Although immunosuppressive drugs can prevent graft rejection to a certain degree, their efficacies are limited, transient, and associated with severe side effects. Induction of thymic central tolerance to allografts remains challenging, largely because of the difficulty of maintaining donor thymic epithelial cells *in vitro* to allow successful bioengineering. Here, the authors show that three-dimensional scaffolds generated from decellularized mouse thymus can support thymic epithelial cell survival in culture and maintain their unique molecular properties. When transplanted into athymic nude mice, the bioengineered thymus organoids effectively promoted homing of lymphocyte progenitors and supported thymopoiesis. Nude mice transplanted with thymus organoids promptly rejected skin allografts and were able to mount antigen-specific humoral responses against ovalbumin on immunization. Notably, tolerance to skin allografts was achieved by transplanting thymus organoids constructed with either thymic epithelial cells coexpressing both syngeneic and allogenic major histocompatibility complexes, or mixtures of donor and recipient thymic epithelial cells. Our results demonstrate the technical feasibility of restoring thymic function with bioengineered thymus organoids and highlight the clinical implications of this thymus reconstruction technique in organ transplantation and regenerative medicine.

Received 30 July 2014; accepted 5 April 2015; advance online publication 16 June 2015. doi:10.1038/mt.2015.77

INTRODUCTION

The primary function of the thymus is to continuously generate a diverse population of T-cells that can elicit adaptive immune responses against invading pathogens while promoting self-tolerance.[1] The thymus is a rather vulnerable organ as many factors, including environmental insults, aging, genetic composition, virus infection, irradiation, and anticancer drug treatments, which can all irreversibly compromise its function.[2,3] Impaired immune surveillance consequent to thymic dysfunction leads to diseases ranging from autoimmunity to immunodeficiency and malignancy.[4]

The thymus is organized into two morphologically and functionally distinct compartments: the cortex and the medulla, which house two distinct populations of thymic epithelial cells (TECs): the cortical TECs (cTECs) and the medullary TECs (mTECs).[5–8] Other thymic stromal cells (TSCs) include thymic fibroblasts, endothelial cells, as well as antigen presenting cells (APCs) like macrophages and dendritic cells (DCs). Overall, this network of thymic cells provides both homing signals for the immigration of lymphocyte progenitors originated from the bone marrow (BM) and trophic factors necessary for the differentiation and maturation of thymocytes.[9]

Although numerous efforts have been made to correct thymic defects, manipulating the thymus, either *in vitro* or *in vivo*, proves to be challenging. This is mainly attributed to the unique architecture of the thymic stroma that is essential for the maturation, survival, and function of TECs. Unlike epithelial cells of other visceral organs, which form a two-dimensional (2-D) sheet-like structure on the basement membrane to create borders within and between organs,[10] TECs form a sponge-like three-dimensional (3-D) network that is essential for their function.[11] TECs cultured on irradiated 3T3 feeders (a 2-D environment) are unable to support T-cell differentiation from lymphocyte progenitors, but start to express markers of terminally differentiated epithelial cells.[12] Recently, TEC stem cells derived from early embryos were shown to differentiate into skin cells when cultured in 2-D environment.[13] Indeed, the expression of key genes for the specification and proliferation of TECs (*e.g.*, FoxN1, DLL-4, CLL-22 and Tbata) are shown to be dependent on the 3-D organization of the thymic stroma, further indicating that the unique microenvironment of the thymus is essential to maintain the unique property of TECs to support T lymphopoiesis.[14]

Over the years, substantial progress has been made to reproduce the thymic microenvironment. Matrigel and other

Correspondence: Massimo Trucco, Institute of Cellular Therapeutics, Allegheny Health Network, 320 East North Avenue, 11th Floor, South Tower, Pittsburgh, PA 15212, USA. E-mail: mtrucco1@wpahs.org

collagen-based synthetic matrices were shown to be able to support limited differentiation of lymphocyte progenitors into T-cells.[15,16] TECs cultured in artificial 3-D matrix are viable and can partially support thymocyte development. Recently, Pinto *et al.* developed a coculture system, in which mTECs were layered on top of a 3-D artificial matrix embedded with human skin-derived dermal fibroblasts. Under such conditions, mTECs can retain some of their key features (*e.g.*, expression of FoxN1, Aire, and tissue-specific antigens).[17] In a similar approach, Chung *et al.* mixed TECs and thymic mesenchyme, both isolated from postnatal human thymi, with CD34$^+$ cells from cord blood to form implantable thymic units.[18] The thymic microenvironments of these thymic reaggregates can support thymopoiesis *in vitro* and are able to generate a complex T-cell repertoire when transplanted in nonobese diabetes (NOD).scid gamma humanized mice *in vivo*. However, to date, none of these approaches has been able to fully recapitulate the function of a thymus.

Recently, significant advances have been made in "cell-scaffold" technology.[19] This groundbreaking technology uses a detergent-perfusion based approach that allows the clearance of the cellular constituent of almost any organ of any scale, while retaining its original 3-D architecture and extracellular matrix (ECM) components.[20,21] Repopulating the decellularized natural scaffolds with tissue-residing mature cells or progenitor/stem cells can promote its recellularization and partially recover organ function.[22] To date, these "cell-scaffolds" have been primarily applied to manufacture and implant relatively simple organs, such as tissue engineered vascular grafts and skin, with some success.[23–25] Regeneration of complex organs such as liver, heart, lung, and kidney has also been attempted in animal models.[21,26–29] Although limited, encouraging functional regeneration of the engineered organs was observed. Furthermore, a successful clinical implantation of reconstructed decellularized trachea underlines the clinical potential of this technology.[30]

Here, the authors show that thymus organoids reconstructed with the "cell-scaffold" technology can support thymopoiesis *in vivo* to establish both humoral and cellular adaptive immunity in athymic nude mice. In addition, they also induce central immune tolerance to allo-skin grafts.

RESULTS

Bioengineering thymus organoids with decellularized thymus scaffolds

To investigate the possibility of reconstructing viable thymus organoids with TECs, the authors developed a thymus decellularization protocol improvised from an earlier approach described for embryoid bodies.[22,31,32] This allowed us to remove all the cellular elements of a mouse thymus while maintaining all the major ECM components (**Figure 1a–d**). Scanning electron microscopy (SEM) analysis of the cross-section images of the acellular thymic scaffolds revealed the preservation of ECM micro structures (*e.g.*, grooves, ridges, and the fibrillar meshwork), indicating that the 3-D architecture of thymic stromal ECM is largely intact following the decellularizing treatment (**Figure 1e**).

CD45$^-$ TSCs, including TECs, endothelial cells and thymic fibroblasts (see **Supplementary Figure S1a**), were harvested from 3–4 weeks old mice and were injected into the decellularized scaffolds and cultured in the top chamber of transwells. Because previous studies have shown that cross talk between TECs and the developing thymocytes is essential for their mutual survival and proliferation,[2] lineage marker negative (Lin$^-$) progenitor cells from BM were cointroduced into the thymus scaffolds to mimic the immigration of lymphocyte progenitors (**Figure 2a** and see **Supplementary Figure S1b,c**). In striking contrast to the rapid loss of adult TSCs in hanging drop culture, or in porous disk on a gel foam routinely used for *in vitro* fetal organ cultures, TSCs remained viable for >3 weeks in the 3D-thymic scaffolds (**Figure 2b,c** and see **Supplementary Videos S1 and S2**). Of note, 7 days after thymus reconstruction, some of the injected stromal cells began to assume a fibroblast-like morphology, suggesting that these cells successfully colonized the 3D ECM (**Figure 2b**). Immunohistochemical analysis of reconstructed thymus organoids cultured *in vitro* showed the presence of both TECs and CD45$^+$ lymphoid cells (**Figure 2c**, *left* panel; see **Supplementary Figure S2 and Supplementary Video S3**). Thymic "nurse" cells, the subset of cTECs that envelop multiple CD4$^+$CD8$^+$ double positive thymocytes within its intracellular vesicles to support their T-cell receptor (TCR) selection and survival, were also present, suggesting that the reconstructed thymus organoid can at least retain some of its supportive properties of T lymphopoiesis *in vitro* (**Figure 2c**, yellow arrow in *right* panel). Furthermore, Ki67$^+$Epcam$^+$ TECs within the 3-D scaffolds were also observed, suggesting their proliferative potential (**Figure 2c**, red arrow in the *right* panel). These data are consistent with earlier findings that there exist progenitor cells of the thymic epithelia in the adult thymus.[33] In addition, other TSCs such as CD31$^+$ endothelial cells and thymic fibroblasts were also present, suggesting that the 3-D scaffold microenvironment is suitable for the survival of various TSC types (**Figure 2d**).

Under 2-D culture conditions, TECs rapidly lose their signature gene expression and upregulate the expression of markers of terminally differentiated skin epithelial cells.[17] Simultaneously, they also lose their capability to positively and negatively select developing thymocytes. In contrast, transcription of TEC-specific genes was readily detectable in the reconstructed thymus organoids cultured for 7 days *in vitro* (**Figure 2e**). These included the widely used thymic epithelium marker EpCAM, and the transcription factor Foxn1, which regulates the expression of a number of key factors in TECs (*e.g.*, *Dll4*) that are essential for thymopoiesis. Transcripts of *Ccl25*, a downstream target of Foxn1 that promote the homing of hematopoietic progenitors in the thymus, were also present in the thymus organoids.[34] In addition, both *Krt5* and *Krt8*, the cytokeratins predominantly present in mTECs and cTECs, respectively, were expressed, suggesting that both cTECs and mTECs were present. Interestingly, factors that can modulate TEC proliferation (*e.g.*, *Trp63* and *Tbata*) were also expressed in cells of the bioengineered thymus.

Another signature feature of mTECs is their capability to ectopically express tissue-specific antigens, believed to be a key part of the central mechanism to distinguish self from nonself and establish immune tolerance to peripheral tissues and organs.[35,36] mRNA transcripts of *Aire*, one of the key regulators of thymic tissue-specific antigen expression, were present in TSCs of the thymus organoids, in conjunction with both Aire-dependent

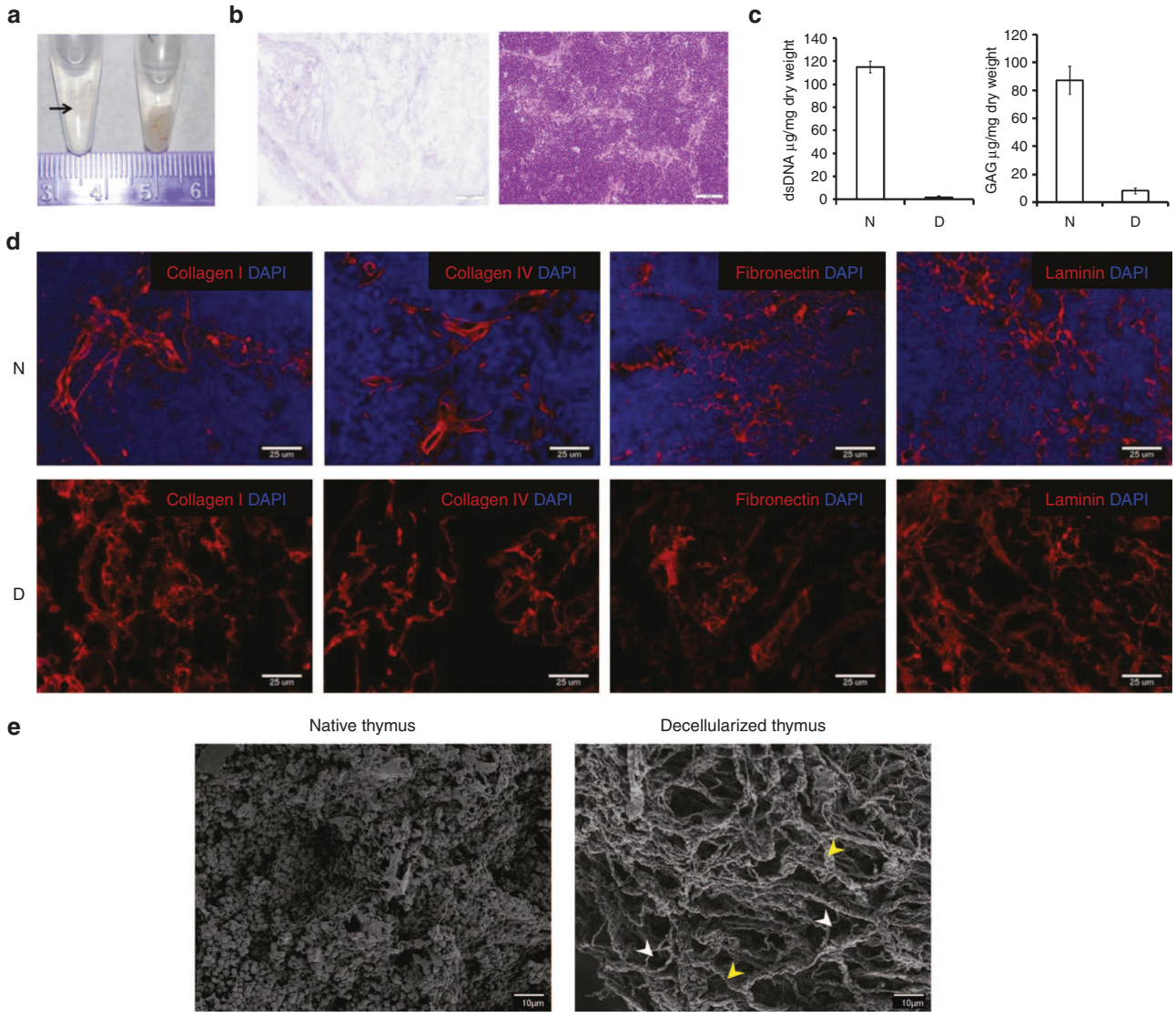

Figure 1 Preservation of 3-D ECM architecture in decellularized mouse thymus scaffolds. (**a**) Mouse thymus was decellularized with detergent and preserved in PBS. D, decellularized thymus (arrow); N, naive thymus. (**b**) H&E images of 7um paraffin sections of decellularized thymus scaffolds (D, *left panel*) and naive thymus (N, *right panel*). No remnant cell is detected after the completion of decellularization. White scale bar, 50 µm. (**c**) *Left panel*, Picogreen analysis of DNA contents in decellularized thymus scaffolds (D, $n = 3$), showing the removal of up to 99% of DNA materials, in comparison to the naive thymi (N, $n = 3$). *Right panel*, glycosaminoglycan (GAG) content in the decellularized thymus scaffolds. About 7.5% of sulfated GAG contents are preserved in the scaffolds. (**d**) Immunohistochemical analysis of the preservation of the extracellular matrix (ECM) components (red) in the thymus scaffolds. Cryosections of naive thymus (N, *upper* panels) and decellularized thymus scaffolds (**d**, *lower* panels) were stained with antibodies against ECM proteins (*red*, Collagen I, Collagen IV, fibronectin, and laminin), and counterstained with DAPI (4′,6-diamidino-2-phenylindole) for nucleus (blue). (**e**) Ultrastructure characterization of native and decellularized thymus. *Left panel*, representative scanning electron microscopy (SEM) image of native thymus (N) showing distinct individual cells. *Right panel*, SEM image of decellularized thymus (D) shows the preservation of 3D meshwork within the parenchymal space composed of variety of fibers, including large bundle of Type I collagen (yellow arrowhead) associated with a variety of smaller fibers (white arrowhead). No cell is detected throughout all tissue layers, indicating complete removal of the cellular components.

(*e.g.*, *Ins2*)[32] and Aire-independent (*e.g.*, *Ica1*)[37] tissue-specific antigens (**Figure 2f**). The persistence of TEC marker expression in the thymus organoids after extensive *in vitro* culture (**Figure 2f**) also suggests that the thymic scaffold microenvironments might support the survival of thymic epithelial progenitor cells. Although embryonic thymic epithelial progenitor cells are much better defined (MTS20$^+$MTS24$^+$Plet-1$^+$),[7,8,38,39] markers of their adult counterparts remain unclear. Recently, Wong *et al.* identified a subset of TECs (EpCAM$^+$ MHCII^{lo}UEA^{lo}, designated as TEC^{lo}) in adult mouse that display properties of thymic epithelial progenitor cells, including self-renewal and capability to differentiate into multiple TEC lineages.[40] The authors examined the presence of TEC^{lo} cells in the reconstructed thymus organoids after 12 days of *in vitro* culture and found comparable frequencies of the TEC^{lo} population as those of the initial input (see **Supplementary Figure S3**). Overall, these findings suggest that the 3-D scaffold environment of the decelluarized thymus can support the long-term survival of TECs *in vitro* and enable them to retain the thymic specific patterns of molecule expression that is essential for T-cell development.

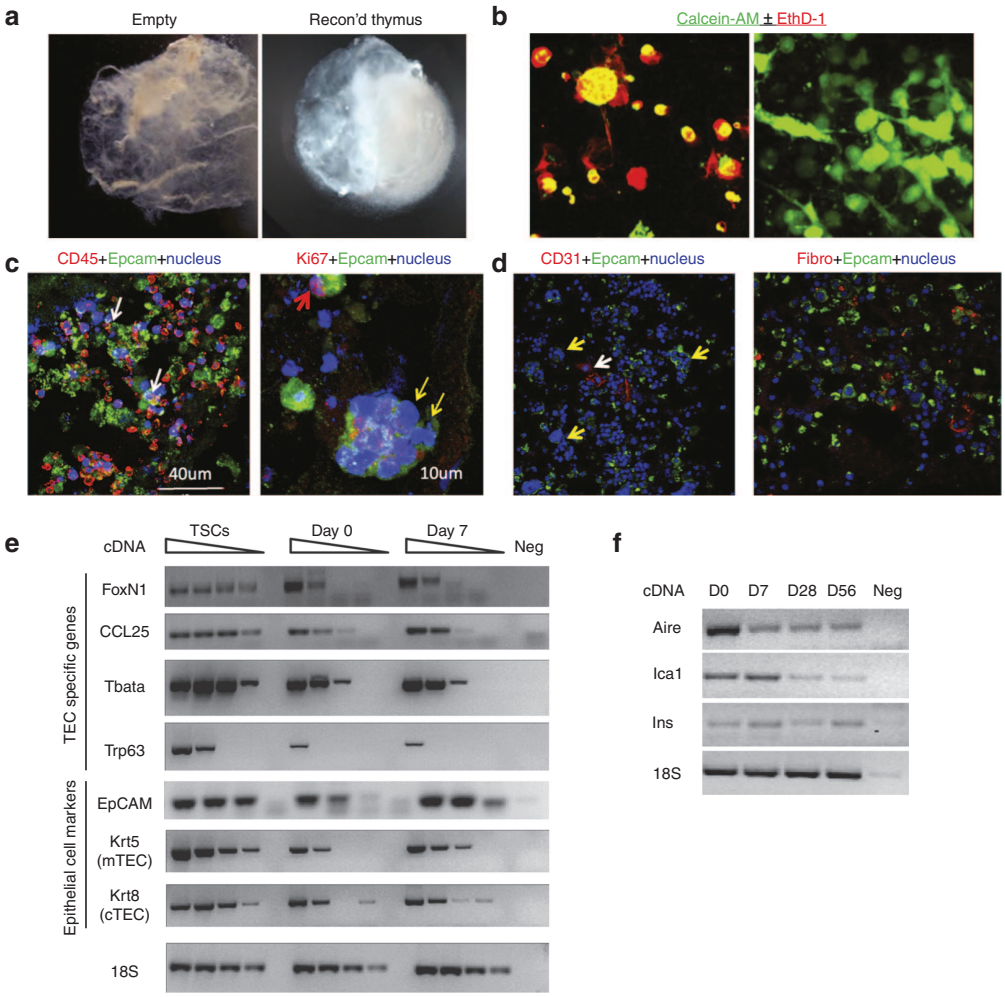

Figure 2 Reconstruction of thymus organoids from decellularized thymus scaffolds. (**a**) Light microscopic images of a decellularized thymus scaffold (*left* panel) and a reconstructed thymus organoid (with CD45⁻ thymic stromal cells and bone marrow cells of Lin⁻ population at 1 : 1 ratio) cultured overnight *in vitro* (*right* panel). (**b**) Fluorescent microscopic images of thymic stromal cells (TSCs) cultured either as "hanging drop" overnight (*left* panel) or in the 3-D scaffold for 7 days (*right* panel). Live cells were discriminated from the dead cells by their intracellular esterase activities to generate green fluorescent calcein-AM (green) and their capabilities to exclude the red-fluorescent ethidium homodimer-1 (EthD-1, red) from entering the nucleus. (**c,d)** Representative immunohistochemical images of reconstructed thymus organoids cultured *in vitro* for 7 (**d**) or 21 (**c**) days. (**c**) Cryosections were stained with antibodies against Epcam (green), counterstained with either anti-CD45 (red, *left* panel) or anti-Ki67 (red, *right* panel) antibodies. In the left panel, white arrows show the presence of close interactions between the CD45⁺ thymocytes and the Epcam⁺ thymic epithelial cells (TECs). In the right panel, the yellow arrows show the presence of multicellular thymus nurse cell complex, whereas the red arrow shows a Ki67⁺Epcam⁺ TEC. (**d**) Cryosections were stained with endothelial cell-specific anti-CD31 antibodies (red, left panel) and fibroblast-specific antibodies (red, fibro, right panel). Both sections are counterstained with the anti-Epcam antibodies (green) and the Hoechst 33342 dye (blue) for TECs and nuclei, respectively. (**e**) Semiquantitative RT-PCR analyses of CD45⁻ thymic stroma specific gene expression in TSCs, reconstructed thymus organoids cultured *in vitro* for 0 and 7 days (day 0 and day 7, respectively). Sample dilutions: undiluted, 1/4, 1/16, and 1/64. (**f**) RT-PCR analyses of tissue-specific antigen transcription in reconstructed thymus organoids cultured *in vitro* for 0, 7, 28, and 56 days. All the experiments were repeated at least once with similar results.

To examine whether the ECM microenvironment of the reconstructed thymus organoids can support T-cell lineage determination and differentiation *in vitro*, Lin⁻ BM progenitors were isolated from C57BL/6 mice (of CD45.2 allelic type) and mixed with TSCs harvested from C57BL/6.CD45.1 congenic mice (designated as B6.CD45.1 hereinafter) at 1 : 1 ratio. The reconstructed thymus organoids were cultured *in vitro* for 9 days, in the presence of recombinant interleukin-7, and the differentiation of CD45.2⁺ BM progenitors into T-cell lineages was examined with flow cytometry (FCM). CD3 was expressed in ~10% of the CD45.2⁺ cells, which include both double positive (DP, CD4⁺CD8⁺) and single positive (SP, CD4⁺CD8⁻ or CD4⁻CD8⁺) thymocytes (see **Supplementary Figure S4**). Even though further optimization of the conditions is needed, the results suggest that the reconstructed thymus organoids can support the development of T-cells *in vitro*.

Bioengineered thymus can support T lymphopoiesis *in vivo*

The capability of the bioengineered thymus to support effective thymocyte development and maturation *in vivo* was examined with transplantation experiments. Thymus organoids reconstructed with mixtures of TSCs and Lin⁻ BM progenitors at 1 : 1 ratio, both harvested from B6.CD45.1 mice, were transplanted

underneath the kidney capsules of B6.nude athymic recipients (designated as Tot.B6.nude for thymus organoid transplanted B6.nude mice hereinafter). Homing of hematopoietic progenitors to the thymus is an intermittent, gated process, alternating between ~1 week of receptive period and ~3 weeks of refractory period.[41,42] The complement of BM progenitors was used to ensure the continuity of cross talk between TECs and the developing thymocytes that is essential for the survival of TECs, at the early post-transplantation stage. The origins of the T-cells in the periphery were identified by FCM analysis of the CD45 congenic markers (*i.e.*, CD45.1 and CD45.2 for donor and recipient origins, respectively).

From 8 weeks postoperative, populations of CD3+CD4+ and CD3+CD8+ T-cells can be clearly detected in circulation and gradually increased over time (**Figure 3a**,**b**). FCM analyses showed that secondary lymphoid organs (*e.g.*, spleen and lymph nodes) were populated with TCRαβ$^+$ T-cells. Both CD4$^+$ and CD8$^+$ T-cells were present, and many displayed similar ratios as immunocompetent naive B6 mice (**Figure 3c**). To ascertain the diversities of T-cell repertoires in the Tot.B6.nude mice, the authors analyzed the distribution of TCR Vβ subtypes in T-cells isolated from the spleens, with a panel of antibodies specific to each Vβ subtype. Similar diversities of Vβ usage were observed between the naive B6 mice and the Tot.B6.nude mice (see **Supplementary Figure S5**). To further assess the diversity of T-cells generated from the reconstructed thymus organoids, the authors performed next-generation-sequencing-spectratyping analysis, which employs high coverage Roche/454 sequencing of TCR (β)-chain amplicons.[43] Broad spectra of Vβ gene families were observed, suggesting that the T-cell repertoire was quite diverse (**Figure 3d** and see **Supplementary Figure S6**). Notably, >99% of the T-cells were CD45.1$^-$CD45.2$^+$, indicating their recipient origins (**Figure 3e**). Overall, these results suggested that the bioengineered thymus organoid constructed from adult TSCs could effectively attract the homing of lymphocyte progenitors from the recipient's BM and supported the development of a diverse T-cell repertoire.

The majority of the CD8+ T lymphocytes in the spleens of Tot.B6.nude mice displayed a CD62L^{high}CD69^{low} phenotype, suggesting that they were naive cells, whereas the percentages of CD4$^+$ T-cells with activated phenotype was higher than naive B6 mice (**Figure 3f**). This might be the natural response of newly generated T-cells under lymphopenic conditions.[44] Nevertheless, neither thymus-reconstructed mice displayed any pathological sign of autoimmunity, nor did the authors observe any lymphocytic infiltration in various solid organs with histology analysis (*e.g.*, liver, pancreas, heart, etc.; data not shown). The percentages of regulatory T-cells in the spleens of transplanted nude mice were similar to those of naive B6 controls (**Figure 3g**), consistent with a self-tolerant T-cell repertoire. Furthermore, the CD4$^+$CD25$^+$Foxp3$^+$ regulatory T-cells were predominantly positive for Helios, a marker for naturally occurring regulatory T-cell subset,[45] suggesting that they most likely originated from the transplanted thymus organoids (**Figure 3h**).

Immunohistochemical examination of the thymus organoid grafts 16 weeks post- transplantation showed the presence of EpCAM$^+$ TECs, as well as CD4$^+$ and/or CD8$^+$ thymocytes underneath the kidney capsules (**Figure 3i**). These results further suggested that the thymus organoid grafts can support the survival and function of the TECs, but also promote the homing and differentiation of lymphocyte progenitors *in vivo*.

Effective cellular and humoral adaptive immunity mediated by T-cells matured in bioengineered thymus organoids

Proliferation under various stimuli has been widely used as a tool to assess the functionality of T lymphocytes. To demonstrate that T-cells derived from the reconstructed thymus organoids are functionally competent, the authors labeled them with carboxyfluorescein diacetate succinimidyl ester (CFSE) and stimulated them with anti-CD3 antibodies. Similar to T-cells of naive B6 mice, a significant percentage of T-cells underwent division, as indicated by dilution of CFSE signals (**Figure 4a**). To further test the function of T-cells derived from the reconstructed thymi, the authors performed mixed leukocyte reaction experiments to evaluate their responses to alloantigens. Proliferation responses similar to those of wild-type B6 mouse were observed, indicating that these T-cells were capable to react to alloantigens (**Figure 4b**). Overall, these results demonstrated that T-cells matured in the transplanted thymus organoids were capable to response to TCR stimulation.

To demonstrate that T-cells derived from the bioengineered thymus can effectively mediate cellular immune response *in vivo*, the authors performed allo-skin transplantation experiments to examine whether the recipients can reject skin allografts. Allogeneic skin grafts harvested from CBA/J mice (H-2^k) were transplanted to the back of Tot.B6.nude mice (n = 3). Syngeneic skin grafts from B6 mice (H-2^b) were cotransplanted as controls. Although the syngeneic skin grafts were well tolerated, the allogeneic skins were rejected within 2–3 weeks, with kinetics similar to naive B6 recipient controls (n = 4) (**Figure 4c**). In contrast, allogeneic skin grafts on B6.nude mice that had been transplanted with decellularized empty scaffolds were viable for >8 weeks (**Figure 4d**,**e**). These results demonstrated the capability of T-cells in the Tot.B6.nude mice to efficiently mediate rejection of allogeneic skin grafts while being unresponsive to self-tissues.

One of the essential roles of T-cells in adaptive immunity is their helper function for humoral immunity, namely to mediate immunoglobulin (Ig) class switch in antibody producing B-cells. To examine whether T-cells from the bioengineered thymus can provide helper function to humoral responses, the authors immunized thymus recipients with chicken ovalbumin (OVA), a T-cell-dependent antigen commonly used for studying antigen-specific immune responses in mice. As expected, high titers of anti-OVA antibodies were detectable by ELISA in sera of B6 mice 4–6 weeks postimmunization (**Figure 4f**). Comparable levels of anti-OVA IgG isotypes (*i.e.*, IgG2b and IgG3) were found in serum samples harvested from the Tot.B6.nude mice, whereas seroreactivities against OVA remained at the background levels in immunized B6.nude mice transplanted with empty thymus scaffolds (**Figure 4f**). These results suggest that T-cells generated from the thymus organoids can support B-lymphocyte Ig class switch to mount efficient humoral responses.

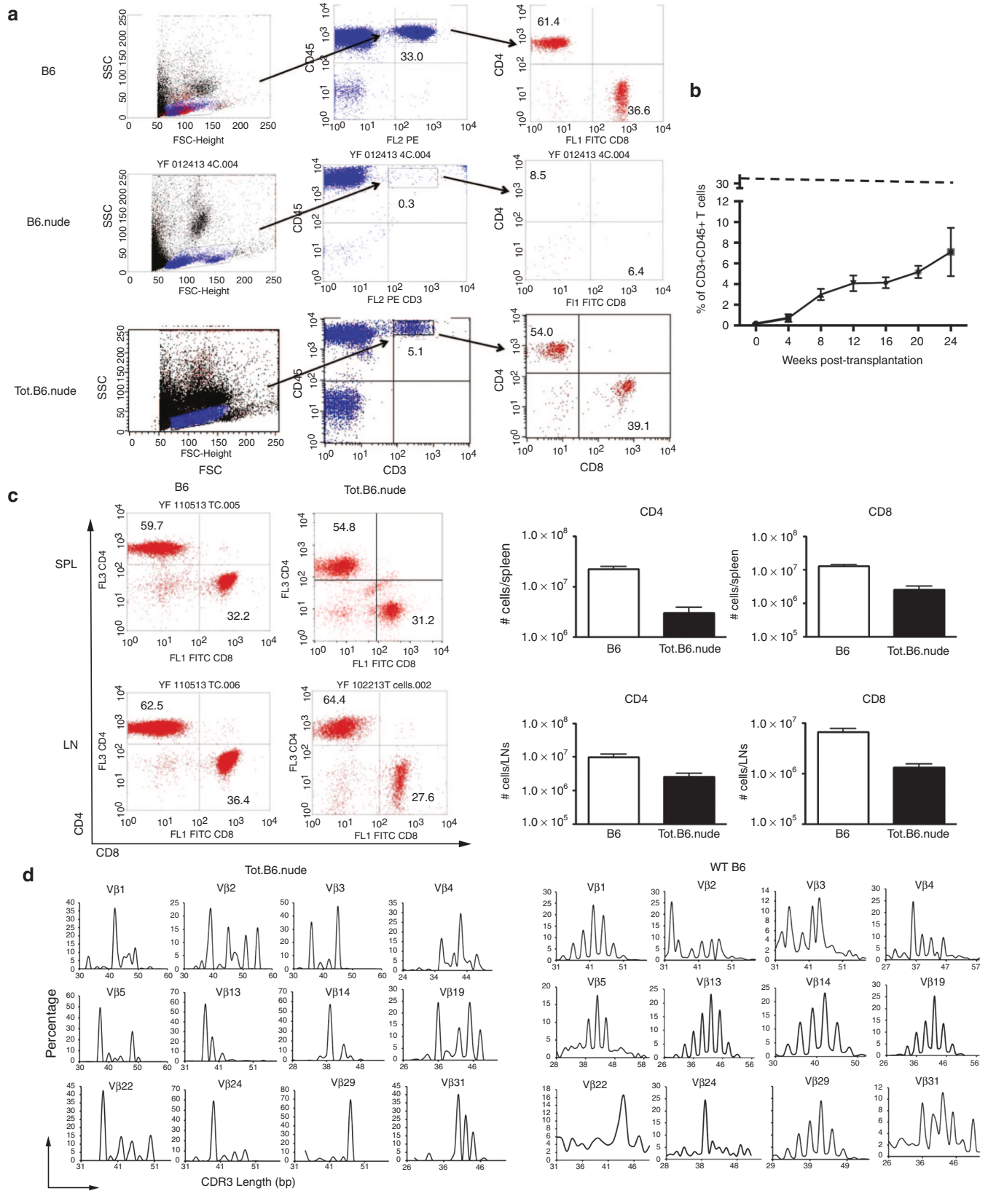

To further demonstrate that T-cells matured in the thymus organoids can elicit antigen-specific adaptive immune responses, Tot.B6.nude mice were immunized with OVA peptide (AVHAAHAEINEAG*SIINFEKL*), which contains an H-2K^b restricted, cytotoxic T lymphocyte (CTL) epitope (the underlined region). Four weeks after the initial vaccination, splenocytes were challenged with the OVA peptide and the presence of T-cells secreting proinflammatory cytokine interferon-γ (IFN-γ)

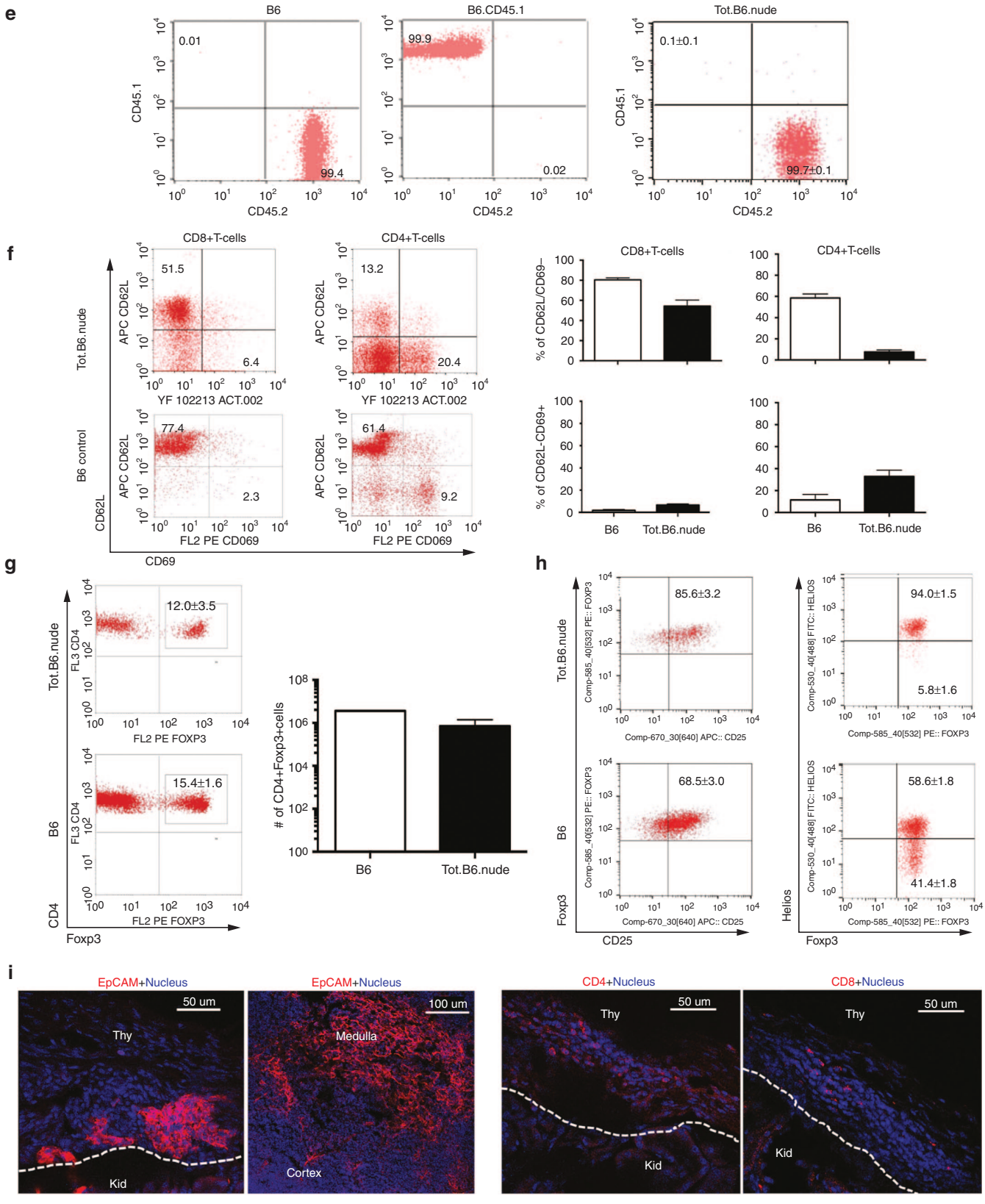

Figure 3 Reconstructed thymus organoids support T lymphopoiesis in athymic hosts *in vivo*. (**a**) Representative flow cytometric (FCM) profiles for both $CD3^+CD4^+$ and $CD3^+CD8^+$ T-cells in the blood circulation of B6.nude mice transplanted with reconstructed thymus organoids (Tot.B6.nude, 16-weeks post-transplantation, *lower panels*), in comparison to the profiles of either the wild-type (WT) C57BL/6 (B6, 16 weeks old, *top* panels) or the athymic B6.nude (16 weeks old, *middle* panels) mice. Numbers indicate the frequencies of cells within the indicated areas. (**b**) Progression of T-cell development in Tot.B6.nude mice. Percentages of $CD3^+CD45^+$ T-cells in peripheral blood leukocytes (PBLs) of Tot.B6.nude mice (n = 4–15)

was evaluated with the Enzyme-Linked ImmunoSpot (ELISPot) assay. As shown in **Figure 4g**, significant numbers of OVA peptide responding cells were present, suggesting that Tot.B6.nude mice can effectively mobilize proinflammatory response on antigen challenge.

Induction of allo-skin tolerance with bioengineered thymus organoids constructed with TECs of F1 hybrid of donor and recipient mice

Achieving donor-specific immune unresponsiveness, without the need for pharmacologic immunosuppression, remains a major goal of transplantation immunological research. To prove the principle that transplantation of bioengineered thymus organoids expressing both donor and recipient major histocompatibility complexes (MHCs) can establish central tolerance to donor antigens, the authors reconstructed the acellular thymus scaffolds with TSCs harvested from the F1 offspring (B6.H-$2^{b/g7}$) of a cross between B6 (H-2^b) and B6.H-2^{g7} congenic mice, and transplanted them to the B6.nude recipients (H-2^b). The B6.H-2^{g7} mouse is a congenic line in which a 19 cM segment of Chr 17 including the MHC of the B6 mouse (of the H-2^b haplotype) was replaced with that of the nonobese diabetes mouse line (of the H-2^{g7} haplotype). It was established through multiple rounds of backcrossing of the NODxB6 F1 mice to the parental B6 line. Once a substantial population of T-cells became detectable (12–16 weeks) in the peripheral bloods of the recipients, skin grafts harvested from both the syngeneic B6 (H-2^b) and the allogeneic B6.H-2^{g7} congenic mice were transplanted on their backs. To demonstrate that the thymus organoid transplanted recipients retained their capabilities to reject third-party alloantigens, skin grafts harvested from CBA/J (H-2^k) mice were also transplanted (**Figure 5a**). Successful engraftments of skin transplants from both the syngeneic B6 and the allogeneic B6.H-2^{g7} mice were observed, whereas the third-party CBA/J skin grafts were rejected within 2–3 weeks (**Figure 5b**,**c**). Immune unresponsiveness to H-2^{g7} alloantigens in the recipients was further demonstrated in mixed leukocyte reaction assays (**Figure 5d**). Overall, these results suggested that transplantation of bioengineered thymus organoids coexpressing both syngeneic and allogeneic MHCs can effectively establish donor-specific immune tolerance.

Induction of allo-skin tolerance with bioengineered thymus organoids constructed with mixture of TECs from both the donor and the recipient

Although reconstructing thymus organoids with TECs coexpressing both donor- and recipient-MHCs can effectively induce tolerance to donor MHC-expressing grafts, it is not clinically feasible to transfer donor MHC genes to the recipient's TECs at such high efficiency (100% in the case of F1 TECs), using currently available gene engineering techniques. Moreover, epitopes derived from mismatched genes other than the MHCs in the allogeneic donor organ(s) can also contribute to its rejection. A possible way to overcome these obstacles is to incorporate the donor TECs in the thymus organoids, together with the recipient's TECs. To test this hypothesis, the authors performed the experiments schematically illustrated in **Figure 6a**. TECs harvested from B6 (H-2^b) and CBA/J (H-2^k) were mixed at 1 : 1 ratio and coinjected with B6 BM progenitors to the decellularized thymus scaffolds. B6.nude mice reconstructed with the thymus organoids were challenged with allogeneic CBA/J skins, as well as skin grafts from the third-party Balb/C mice (H-2^d). Prolonged survival of the CBA/J skin allografts was observed (**Figure 6b**). Consistently, results of mixed leukocyte reaction experiments revealed that when challenged with CBA/J APCs, the levels of T-cell proliferation were significant lower than those stimulated with Balb/C APCs (**Figure 6c,d**). These findings further suggested that including donor TECs in the reconstruction of thymus organoids might be a clinical applicable way to induce donor-specific immune tolerance.

DISCUSSION

The authors provided functional evidence that bioengineered thymus organoids made of decellularized thymic scaffolds populated with TECs and Lin$^-$ BM progenitors can reassert thymic T-cell generation in athymic nude mice. Although attempts to decellularize the thymus glands and repopulate them with epithelial cells have been reported earlier,[46,47] to our knowledge, the

were analyzed by FCM every 4 weeks post-thymus organoid transplantation. Dashed line shows the percentage of T-cells in PBLs of 8-week old, WT B6 mice (33.5 ± 2.2%, $n = 5$). Data were presented as mean ± SEM. (**c**) Analyses of T lymphocytes in Tot.B6.nude mice. Splenocytes and lymph node (LN) cells were stained for CD3, CD45, CD4, and CD8 and were gated on the CD45$^+$CD3$^+$ population. *Left* panels, representative FCM profiles for CD4$^+$ and CD8$^+$ T-cells in the spleens (SPL, *upper* panels) and LNs (*lower* panels) of Tot.B6.nude mice ($n = 5$, 20 weeks postoperatively) and B6 controls ($n = 3$, 8 weeks old). *Right* panels, the total numbers of CD4 and CD8 T-cells in the SPL and LNs of Tot.B6.nude ($n = 5$) and B6 ($n = 3$) mice. Data were presented as mean ± SEM. (**d**) Spectratyping analysis of the CDR3 Vβ regions of mouse T-cells isolated from the SPL of Tot.B6.nude ($n = 3$) and WT B6 ($n = 3$). (**e**) FCM analyses of the origins of peripheral T-cells in Tot.B6.nude mice ($n = 5$). CD4 T-cells harvested from LNs of WT B6 ($n = 3$), B6.CD45.1 congenic ($n = 3$), and Tot.B6.nude mice were stained with CD45.1 and CD45.2 congenic markers. (**f**) FCM analyses of activation status of peripheral CD4 and CD8 T-cells. T-cells harvested from SPL of WT B6 (open bar, $n = 5$) and Tot.B6.nude (filled bar, $n = 5$) mice were stained for CD62L and CD69. *Left panel*, representative dot blots. Numbers in the representative FCM profiles indicate the frequencies of cells within the indicated areas. *Right panel*, percentages of CD8$^+$ (*left columns*) and CD4$^+$ (*right columns*) T-cells displayed naive (CD62L$^+$CD69$^-$, *top panels*) or activated (CD62L$^-$CD69$^+$, *lower panels*) phenotypes. Data were presented as mean ± SEM. (**g**) FCM analyses of the frequencies of Foxp3+ regulatory cells in the CD4 T-cell population. T-cells were harvested from SPL of WT B6 ($n = 5$) and Tot.B6.nude ($n = 5$) mice were stained intracellularly for Foxp3. *Left panel*, representative dot blots of CD4$^+$Foxp3$^+$ regulatory T-cells. Numbers in the representative FCM profiles indicate the frequencies of cells within the indicated areas. *Right panel*, numbers of CD4$^+$Foxp3$^+$ T-cells in the SPL of Tot.B6.nude mice (filled bar, $n = 5$) and WT B6 controls (open bar, $n = 5$). Data were presented as mean ± SEM. (**h**) FCM analyses of CD4$^+$Foxp3$^+$ regulatory cells in the SPL of WT B6 ($n = 5$) and Tot.B6.nude ($n = 5$) mice. Representative dot blots showing CD25 (*left panels*) and Helios (*right panels*) expression in CD4$^+$Foxp3$^+$ regulatory T-cells. Numbers in the representative FCM profiles indicate the frequencies of cells within the indicated areas. Data were presented as mean ± SEM. (**i**) Immunohistochemical analyses of reconstructed thymus organoids. Representative 7 μm cryosections of thymus organoid grafts, harvested from the kidneys of Tot.B6.nude mice (16 weeks postoperatively), were stained for EpCAM (*left top panel*, red), CD4 (*left lower panel*, red), and CD8 (*right lower panel*, red), and counterstained with Hoechst 33342 (blue). Areas of the reconstructed thymus organoid graft (Thy) and the kidney (Kid) were separated by white dotted lines. *Right top panel*, a representative cryosection of a control WT B6 thymus stained with EpCAM (red). All the experiments were repeated at least once with similar results.

authors show that the decellularized thymus scaffolds can support the survival of TECs *in vitro*, and that the bioengineered thymus organoids can successfully support thymopoiesis and T-cell generation *in vivo*.

Induction of donor-specific immune tolerance remains a major challenge in solid organ transplantation. While the rates of acute rejection have decreased significantly over the past 10 years as a result of new immunosuppressive drugs, long-term allograft survival has not correspondingly improved. Conventional pharmacological drugs (*e.g.*, calcineurin inhibitors and corticosteroids) can cause severe side effects including increased risk of cardiovascular death, diabetes, and kidney disease. Even with the development of modern immunomodulatory protocols such as depletion of mature T-cells with antibodies, blockade of costimulatory molecules (*e.g.*, CD28 and CD40L) and promotion of tolerogenic DCs and regulatory T-cells, issues commonly associated with immune suppression (*e.g.*, high risks of opportunistic microbe infection and tumor development) remain unresolved. Notably, these approaches aim to eliminate/suppress mature donor-reactive T-cells in the periphery; none is designed to address the source of the alloreactive T-cells: the thymus. In addition, some of these treatments might hinder the recovery of thymus function, which is a key to re-establish host defense. Our study demonstrated the technical feasibility of establishing functional donor-specific immune tolerance at the central level, by introducing allogenic donor TECs into bioengineered thymus organoids to obviate the need for immunosuppressive drugs to maintain allograft survival.

Targeting the thymus as a means to achieve immune tolerance in organ transplantation is not a novel concept. Komori *et al.* have shown recently that B6 thymus fragments transplanted into the lymph nodes of Balb/C nude mice can support thymopoiesis and induce immune tolerance of B6 skin grafts.[48] Other approaches undertaken to introduce allogeneic antigens in the thymus include directly injecting donor APCs or alloantigen-expressing viral vectors, or establishing mixed chimerism through thymus irradiation in conjunction with BM transplantation.[49–52] However, most of these approaches predominantly affect APCs, especially thymic DCs, which are replenished by fresh immigrating cells of the recipients in <2 weeks. This intrinsic property of fast turnover of thymic APCs could compromise the long-term efficacy of treatment. In contrast, TECs are an integral cell population of the thymic stroma, whose homeostasis is largely maintained through self-renewal. Although their capability to directly present antigens to developing thymocytes is still under debate, recent studies have shown that thymic DCs can readily acquire antigens from mTECs and present them for negative selection. Thus, the

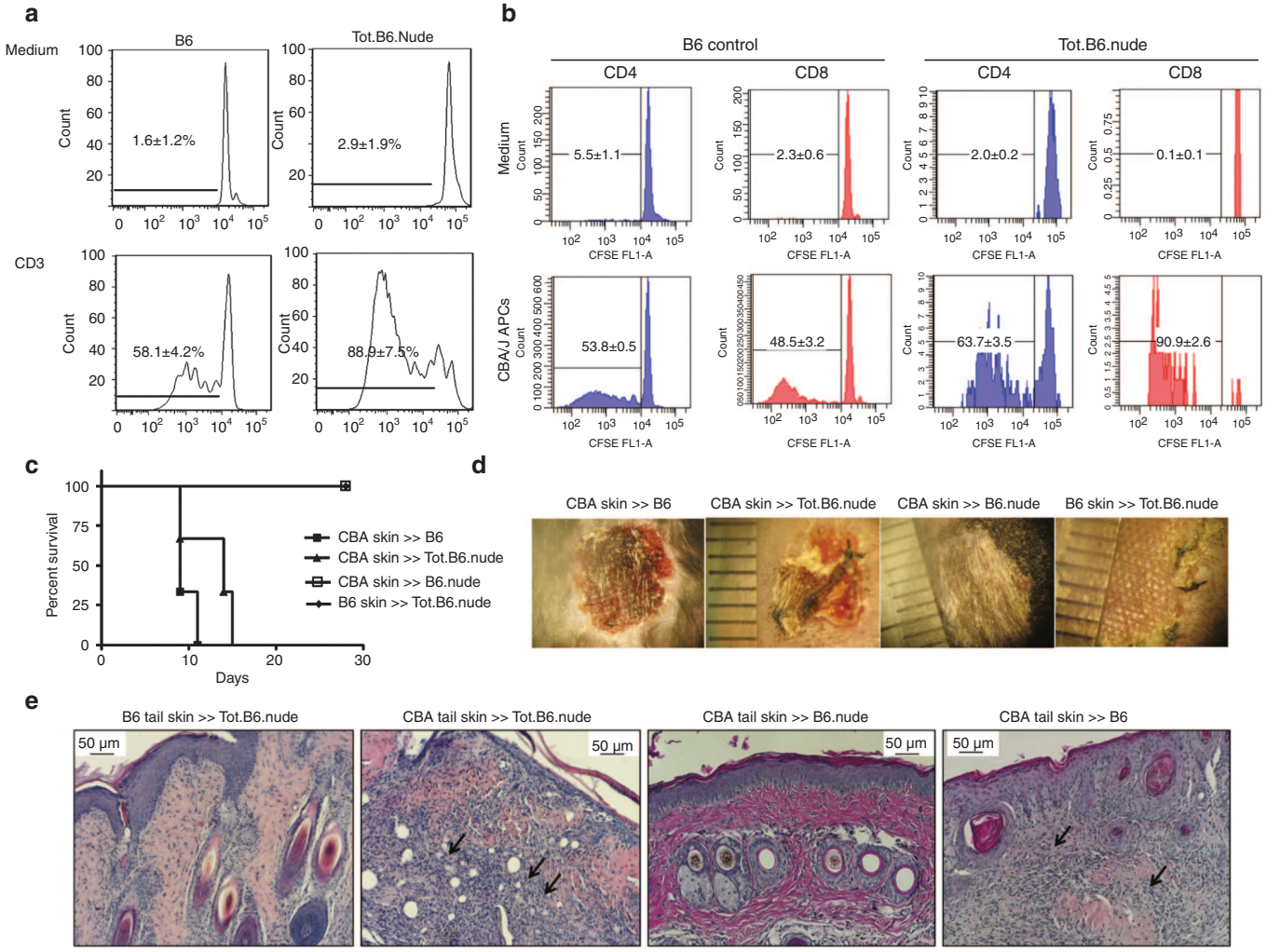

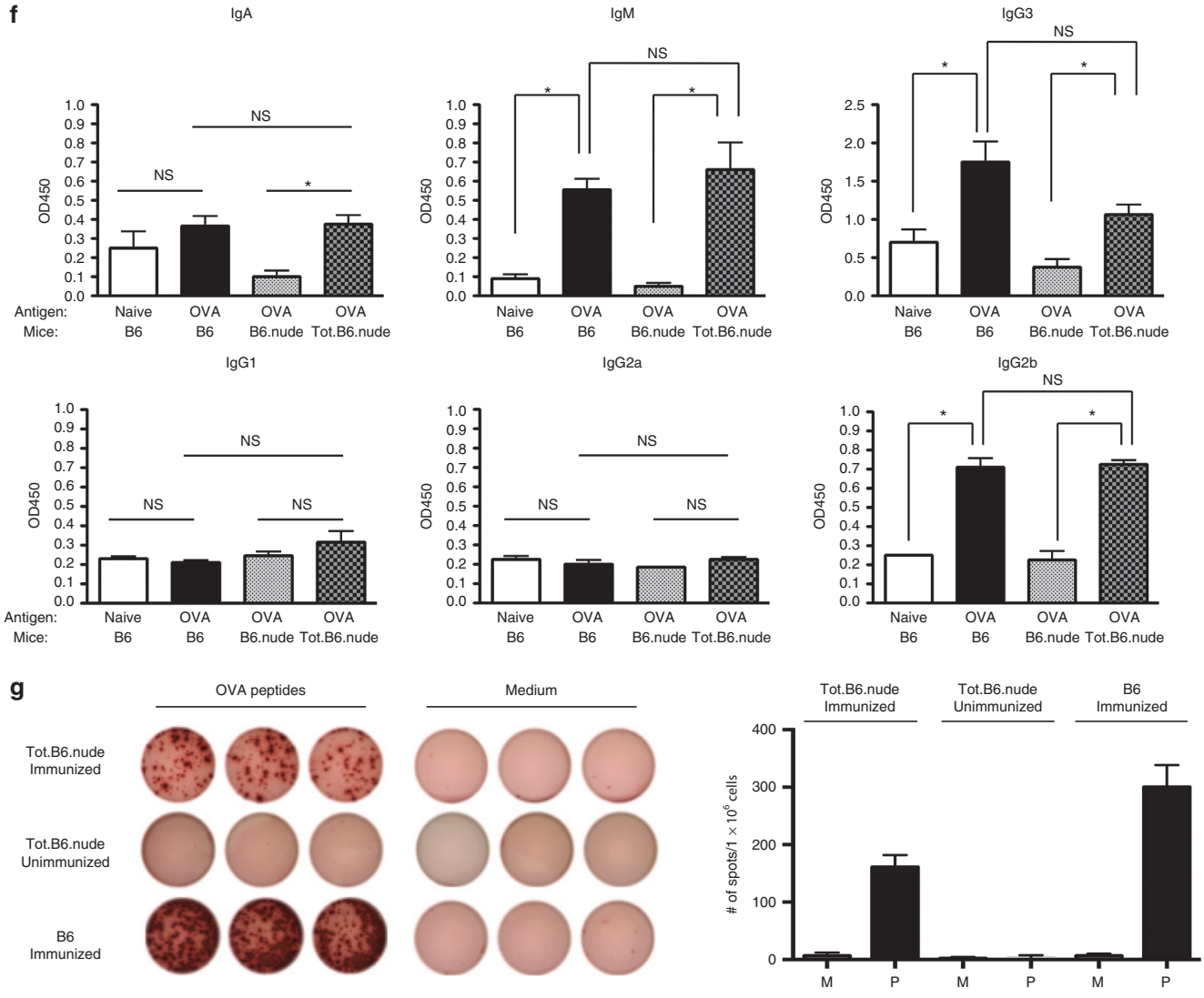

Figure 4 Reconstructed thymus organoids can support T-cell-mediated immunity in athymic hosts *in vivo*. (**a**) Proliferation of T-cells in response to T-cell receptor (TCR) stimulation. T-cells harvested from the spleens of Tot.B6.nude ($n = 4$, *right* panels) and WT B6 mice ($n = 4$, *left* panels) were labeled with carboxyfluorescein diacetate succinimidyl ester (CFSE) and cultured for 7 days in the presence or absence of activating CD3 antibodies. Cells were stained for CD3 and B220, gated on the $CD3^+B220^-$ populations were analyzed by FCM for CFSE levels. All assays were run in triplicate. (**b**) Proliferation of T-cells in response to alloantigens. T-cells enriched from Tot.B6.nude ($n = 4$) and WT B6 mice ($n = 4$) were labeled with CFSE and cultured for 7 days in the presence (*lower* panels) and absence (*upper* panels) of T-cell depleted allogeneic antigen presenting cells (APCs) isolated from CBA/J mice. All proliferation assays were run in triplicate. (**c**) Survival of allogeneic (CBA/J) skin grafts in WT B6 ($n = 3$), B6.nude ($n = 3$), and Tot.B6.nude ($n = 3$) mice, and syngeneic (B6) skin grafts in Tot.B6.nude ($n = 3$). (**d**) Representative photographic images of allogeneic skin grafts in B6, B6.nude, and Tot.B6.nude mice at day 15 post-transplantation. (**e**) Representative histological images (H&E) of paraffin sections of skin grafts harvested from Tot.B6.nude ($n = 4$), B6.nude ($n = 3$), and WT B6 ($n = 3$). Arrows indicate the infiltration of immune cells in the injected skin grafts. (**f**) Analyses of seroreactivities against ovalbumin (OVA) in naive B6 mice ($n = 5$, open bar), B6 mice immunized with OVA ($n = 5$, black bar), B6.nude immunized with OVA ($n = 3$, gray bar), and Tot.B6.nude immunized with OVA ($n = 4$, shaded bar). Levels of OVA-reactive immunoglobulins of various classes and subclasses were determined with ELISA-based, colorimetric assay. NS, not significant; * $P < 0.05$, nonparametric Mann–Whitney test. The assays were repeated twice with similar results. (**g**) Enzyme-Linked ImmunoSpot (ELISpot) analyses of interferon (IFN)-γ-expressing T-cells. Splenocytes harvested from immunized Tot.B6.nude mice ($n = 4$) were challenged with OVA peptides (AVHAAHAEINEAGSIINFEKL). *Left panels,* representative ELISpot images (in triplicate) of splenocytes cultured in presence (*left columns*) or absence (*right columns*) of OVA peptides: *top rows*, immunized Tot.B6.nude mice ($n = 4$); *middle rows*, naive Tot.B6.nude ($n = 3$); lower rows, immunized WT B6 control ($n = 4$). *Right panels*, numbers of IFN-γ-producing spots in the presence of medium (M, open bar) or OVA peptide (P, filled bar). Data were presented as mean ± SEM. The results were obtained from three independent experiments. All assays were run at least in triplicate.

presence of donor antigen-expressing TECs in the bioengineered thymus organoids might ensure the passage of alloantigens to thymic DCs (of the hosts) for negative selection of donor-reactive T-cells, facilitating the establishment of long-term donor-specific immune tolerance.

One of the major challenges to manipulate postnatal TECs for clinical application is their dependency on a properly configured 3-D ECM microenvironment for survival and proliferation. Early studies have shown that thymus fragments cultured in 3-D scaffolds constructed with biocompatible inorganic materials can

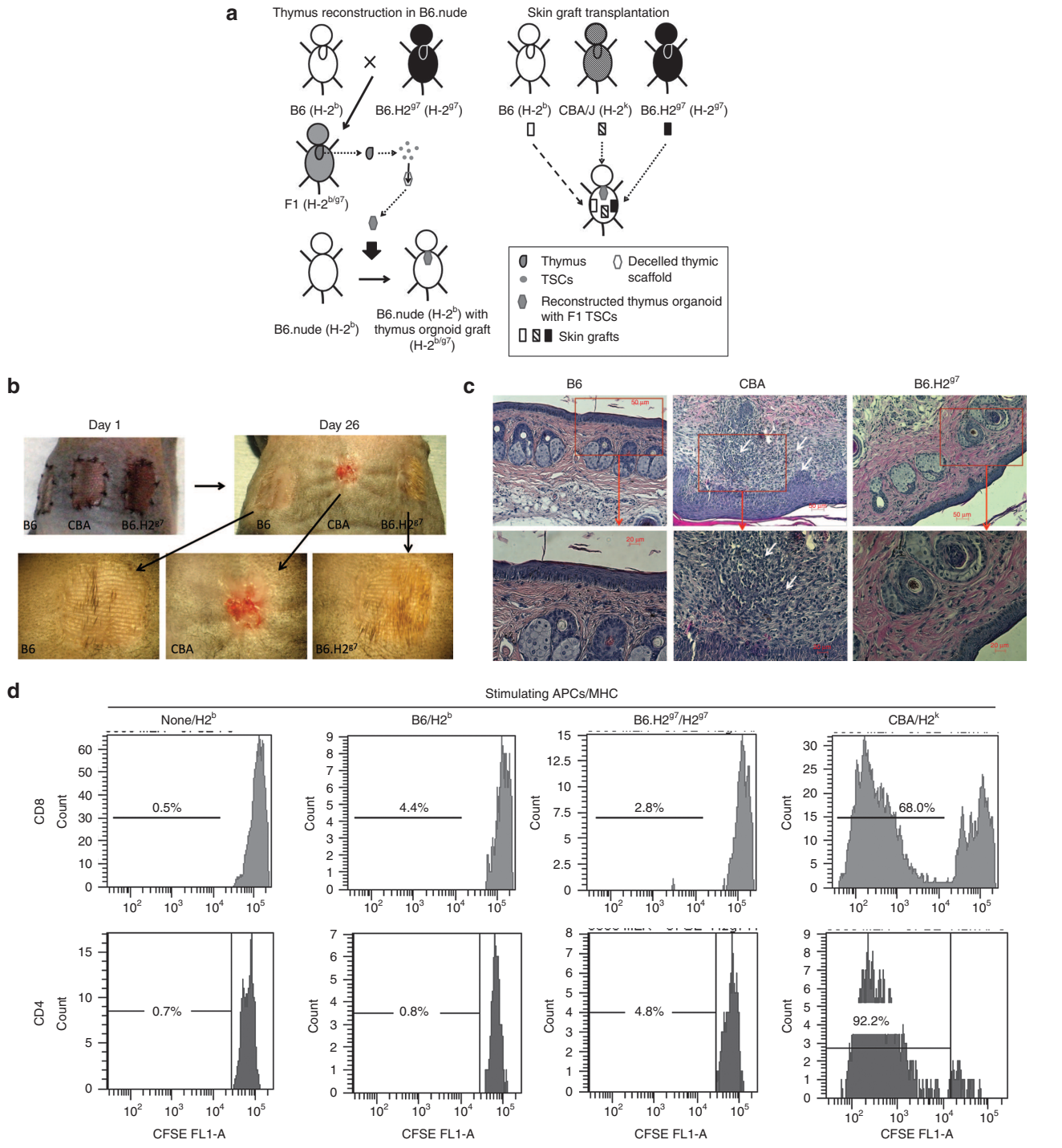

Figure 5 Establishing donor-specific immune tolerance in mouse with reconstructed thymus organoids. (**a**) Schematic outline of strategies to induce immune tolerance of allografts with reconstructed thymus organoid transplantation. Thymus organoids were constructed with thymic stromal cells (TSCs) harvested from F1 offspring of B6 (H-2^b) and congenic B6.H2^{g7} (H-2^{g7}) mice and transplanted to athymic B6.nude mice to generate Tot. B6.nude recipients. Once successful T-lymphopoiesis was demonstrated through flow cytometric (FCM) analyses of peripheral lymphocytes (12–16 weeks post-thymus transplantation), tail skin grafts harvested from wild-type (WT) B6 (syngeneic), congenic B6.H2g7 (allogeneic) and CBA/J (H-2k, third party allogeneic) mice were transplanted to the recipients and were monitored for their survival. (**b**) Representative photographic images of syngeneic (B6) and allogeneic (CBA and B6.H2^{g7}) skin grafts of Tot.B6.nude recipients (n = 4) at day 1 and day 26. Lower panels, higher magnified images of the skin grafts (dotted line) at day 26. Arrows indicate the rejected graft. (c) Representative histological images (H&E) of syngeneic (B6), allogeneic (B6. H2^{g7}), and third-party allogeneic (CBA) skin grafts harvested from Tot.B6.nude recipients (n = 4) at 26 days postskin transfer. Higher magnified images of areas in the red boxes are shown in the lower panels. White arrows show areas with lymphocytic infiltration. (**d**) Proliferation of T-cells of Tot.B6.nude mice (n = 3) in response to alloantigens. T-cells enriched from Tot.B6.nude (n = 3) were labeled with carboxyfluorescein diacetate succinimidyl ester (CFSE) and cultured for 7 days in the presence of T-cell depleted syngeneic (B6), allogeneic (B6.H2g7), and third-party allogeneic (CBA) APCs. Representative FCM results of $CD4^+$ (*left* panels) and $CD8^+$ (*right* panels) T-cells are shown. N/A, no APCs were added to the culture. All proliferation assays were run in triplicate.

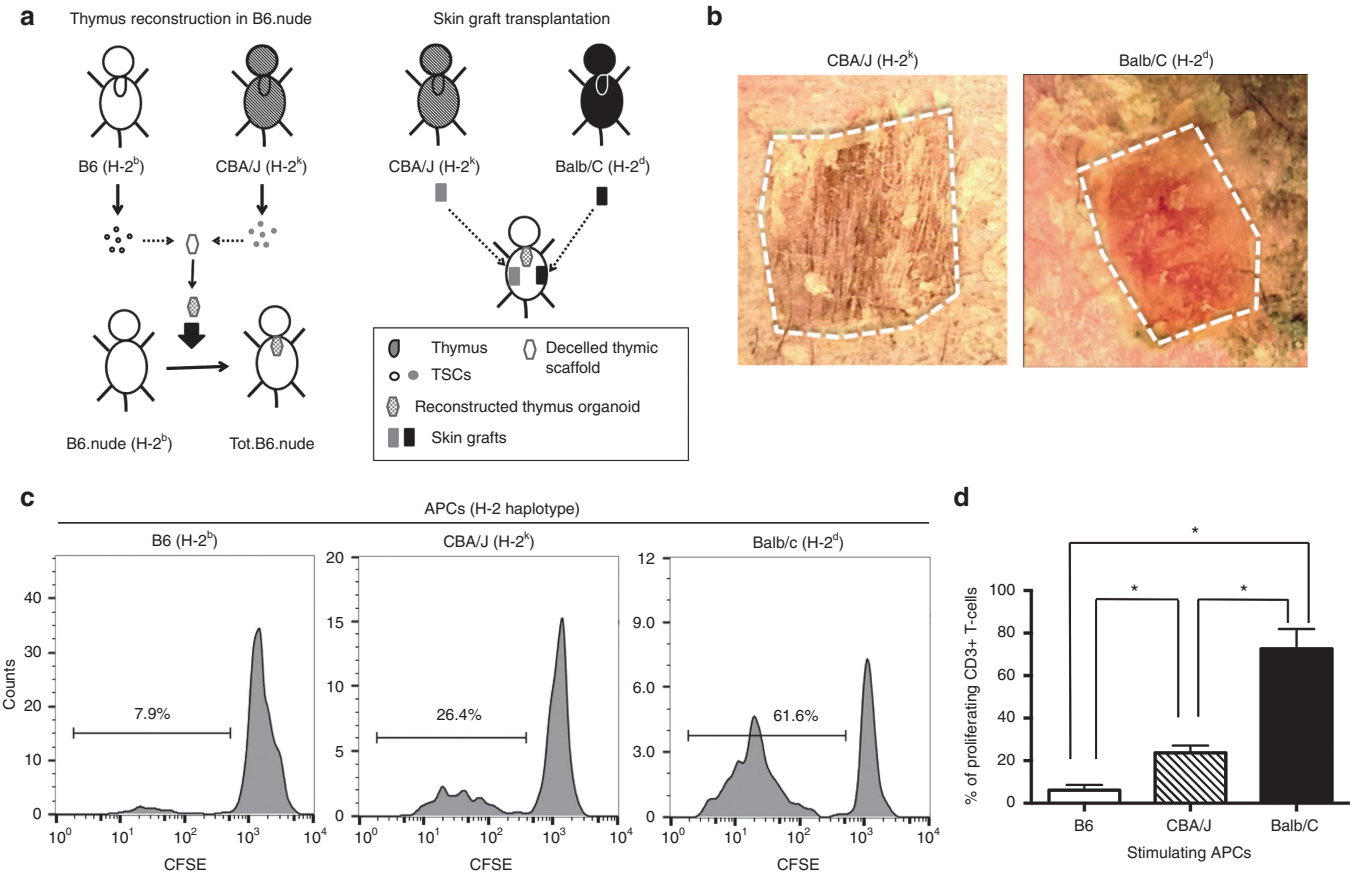

Figure 6 Induction of donor-specific immune tolerance with thymus organoids reconstructed of both donor and recipient thymic epithelial cells (TECs). (**a**) The schematic drawing shows the strategy of the experiment. TECs were isolated from B6 and CBA/J mice and mixed at 1 : 1 ratio. The thymus organoids were reconstructed with B6 Lin-bone marrow progenitors and TECs at 1 : 1 ratio (2×10^5 each), and transplanted underneath the kidney capsules of B6.nude mice. Ten weeks postoperatively, skin grafts harvested from CBA/J and Balb/C (third-party allografts) mice were transplanted to the Tot.B6.nude mice ($n = 4$). Graft survival was monitored for up to 4 weeks. (**b**) Representative photographic images of skin grafts (outlined) on Tot.B6.nude at 22 days postoperatively. While the third-party allograft (*left panel*, Balb/C) is largely rejected, the CBA/J allograft (*right panel*) is well tolerated. (**c**,**d**) Mixed lymphocyte reaction (MLR) experiments, showing the proliferation responses of $CD3^+$ T-cells of the recipient Tot.B6.nude mice ($n = 4$) in the presence of syngeneic or allogeneic APCs. (**c**) Representative carboxyfluorescein diacetate succinimidyl ester (CFSE) dilution histogram: *Left panel*, syngeneic B6 APCs; *middle panel*, CBA/J allogeneic APCs; *right panel*, third-party allogeneic APCs. (**d**) Percentages of proliferating $CD3^+$ T-cells. *$P < 0.05$, nonparametric Mann–Whitney test.

support the differentiation of hematopoietic progenitor cells into $CD3^+$ T-cells.[53] The findings that TECs injected into the thymus scaffolds could retain their specific molecular properties for up to 8 weeks *in vitro* strongly suggested that the 3-D ECM environment of the decellularized thymus provided a suitable and essential niche for the long-term survival of adult TECs. In addition, Lin^- BM progenitors coinjected with the TECs can differentiate into $CD4^+CD8^+$ DP as well as $CD4^+CD8^-$, or $CD4^-CD8^+$ SP thymocytes, suggesting the possibility that with further optimization, the thymus scaffolds could serve as a suitable *in vitro* culture microenvironment to study T-cell development.

Despite the findings that the bioengineered thymus organoids can effectively support T lymphopoiesis and restore thymus functions for both cellular and humoral immunity, the total numbers of T-cells in the spleens of transplanted thymic nude mice were <10% of those of naive B6 mice. Moreover, the T-cell repertoire in the thymus recipients was much less complex than that of naive mice. Many factors might contribute to this inefficiency. For example, thymopoiesis is a well-controlled developmental process, which depends on the cross talk between the developing thymocytes and subsets of TECs in a spatial and temporal manner. Expansion and positive selection of thymocytes occur in the cortical region, whereas final maturation and negative selection of the SP thymocytes predominantly take place in the medulla. Our current top–down approach (breaking up and reassembling) is limited in part by the lack of mechanical control to sort the dissociated cTECs and mTECs into separated functional units. Such lack of proper organization and compartmentalization of TECs might affect the extent of interactions between the developing thymocytes and the thymic stroma, skewing the V(D)J (variable. diversity.joining) recombination events to favor the selection of certain TCRs. Alternatively, deviant thymopoiesis might lead to inefficient output of naive T-cells, resulting in impaired proliferation and over representation of certain early emigrants in the lymphopenic immune environment of the nude mice.

Second, the engraftment site (*i.e.*, kidney capsules) might not be optimal for the survival and function of the thymus organoids. In our studies, intact thymi of 2-week-old mice had largely

degenerated 2–4 weeks after transplantation underneath the kidney capsules (data not shown). One of the major obstacles might be the inefficiency of angiogenesis. To promote graft vascularization, Seach *et al.* embedded thymus fragments in housing chambers consisting of silicone tubing and implanted the device in the vicinity of epigastric blood vessels of nude mice.[54] Although limited, successful T-cell development was observed, and mice were able to reject MHC miss-matched skin grafts. Recently, Chung *et al.* cocultured human postnatal TECs and thymic mesenchymal cells that were transduced with vascular endothelial growth factor-expressing lentiviral vectors, and showed that the engineered human thymic aggregates can support thymopoiesis both *in vitro* and *in vivo*.[18] Refining our thymus bioengineering protocol with these angiogenesis-promoting techniques might enable us to improve survival and the efficacy of the transplanted thymus organoids to support T lymphopoiesis.

To closely mimic the clinical situation, the authors did not use 16-day prenatal mouse embryos to obtain TSCs, but harvested them from 2- to 4-week-old young mice. Although it was demonstrated earlier that a single stem cell from the embryonal region of the thymus can recapitulate the developmental process of the whole thymus organ, and TEC stem cell lines with the potency to differentiate into various TEC subsets have been isolated from 16-day prenatal embryos, the presence and prevalence of multipotent TEC progenitors in a postnatal thymus remain a matter of debate. Consistently, the levels of T-cell development in nude mice transplanted with bioengineered thymus organoids were similar to those transplanted with intact, thymocyte-depleted thymi of 2–4-week-old mice. Thus, the low T-cell numbers in the thymus-transferred nude mice might reflect the intrinsic limitation of the postnatal thymus to fully reconstruct the T-cell repertoire.

Such limitation of postnatal donor TECs (*e.g.*, numbers, regeneration capabilities, and properties) could potentially compromise the efficacy of establishing donor-specific tolerance when the bioengineered thymus is cotransplanted with the solid organ into a transiently immunosuppressed recipient. Especially if the donor is of old age, there might not be enough donor TECs available to completely reconstitute a functional hybrid thymus. Although the factors that can support the survival and proliferation of TEC progenitors remain unknown, a number of cytokines and growth factors (*e.g.*, keratinocyte growth factor, growth hormone, and interleukin-22) have been implicated in maintaining the integrity of thymic stroma, especially the unique characteristics of TECs.[55–58] Recent studies showed that forced expression of the TEC-specific transcription factor FoxN1 could rejuvenate the involuted thymus and increase naive T-cell output in aged mice, suggesting the feasibility of prolonging the function of adult TECs by genetically modulating the expression of key lineage-determining factors in TEC biology.[59,60] Alternatively, donor TECs can be generated from embryonic stem cells,[61,62] induced pluripotent stem cells,[63] or genetically reprogrammed embryonic fibroblasts.[64]

Aided by advances in targeted gene delivery technologies,[65,66] the authors might be able to fine-tune the antigen presentation properties of TECs and bioengineer individualized thymus organoids to achieve long-term donor-specific immune unresponsiveness in clinical transplantation, or to regain self-tolerance to specific tissues in treating autoimmune disorders with known major autoantigen(s). At present, thymus scaffolds can be prepared from thymus glands harvested from cadavers or patients undergoing cardiothoracic surgery in which the thymic samples are removed as waste tissue. As shown in our study, scaffolds prepared from mouse thymi can be stored at 4°C for up to 1 month before use; it is likely that human thymus scaffolds can be preserved in a similar fashion. Because there is no cellular component in the decellularized thymus scaffold, the authors believe that allogeneic (or even xenogeneic) rejection will not be a concern. The thymus organoid can be reconstructed with TECs harvested from the donor and a properly preserved decellularized thymus scaffold from a third party. Indeed, even with the current technology, our preliminary experiments suggest that this thymus bioengineering approach is applicable to nonhuman primates (Fan *et al.*, unpublished observations).

MATERIALS AND METHODS

Mice. All animal protocols were reviewed and approved by the Institutional Animal Care and Use Committee of the Allegheny Health Network (AHN)/Allegheny Singer Research Institute (ASRI). All animals were housed in specific pathogen free environment. The following strains of mice were purchased from the Jackson Laboratory (Bar Harbor, ME): CBA/J, B6 (C57BL/6J), B6.H-2^{g7}, and C57BL/6J.CD45.1 (B6.CD45.1) congenic strain. Athymic B6.nude mice were obtained either from the Jackson Laboratory or from Taconic (Germantown, NY); similar results were obtained from both nude mouse strains.

Skin transplantation. Tail-skin graft was excised from euthanized donor mouse (~1 cm long and 0.5 cm wide) and was placed on a bed prepared by removing an area on the back dermis of either B6.nude or Tot.B6.nude recipient. The graft was sutured, covered with gauze, and was wrapped with sterile bandage. Skin graft survival was monitored daily and rejection was defined as graft necrosis of >80%.

Decellularization of mouse thymus. Decellularization was carried out by chemical detergent washing as mentioned in the earlier study.[22,31] In brief, thymi of 3–4-week-old mice were stored in –80°C till decellularization was initiated. Thymi were thawed in a 37°C water bath. This free-thaw process was repeated three times. Next, ionic detergent, 0.1% sodium dodecyl sulfate (Invitrogen, Grand Island, NY) in deionized water was added to the thymi and placed on a 3-D rotator (Lab Line, Thermo Scientific, Waltham, MA) for continuous rotation till the tissues became translucent and white in color (24 hours). Thymi were subsequently washed in phosphate-buffered saline (PBS) for three times, each for 15 minutes, followed by 30 minutes in 1% Triton X-100 (Sigma-Aldrich, St Louis, MO). This was followed by three more PBS washes. A final wash step of PBS with Pen/Strep (100 U/ml) was added and the scaffolds were rotated for additional 48 hours. The decellularized thymus scaffolds were stored in PBS at 4 °C for up to 1 month and were switched to Roswell Park Memorial Institute (RPMI)-10 culture medium (RPMI-1640 with 10% fetal bovine serum, 100 U/ml Penicillin, 100 µg/ml Streptomycin, 2 mmol/l L-glutamine, 10 mmol/l HEPES) 24 hours before use.

Thymus organoid reconstruction. To reconstruct the thymus organoids, thymic tissue was harvested from 2- to 3-week-old B6 mice, unless specified otherwise, and separated into single cells with collagenase digestion as described earlier.[32,67] In brief, thymic tissue (n = 3–4) was pooled and needle dissected into small pieces of ~1 mm^3, and digested with the Liberase TM solution [0.025 mg/ml Liberase TM (Roche Applied Science, Indianapolis, IN), 0.2 mg/ml DNase I (Roche Applied Science), and 10 mmol/l HEPES in RPMI-1640 (Life Technologies, Carlsbad, CA)] at 37°C for a total of 18 minutes (three rounds of 6 minutes each). All fractions were pooled, incubated with magnetic bead-conjugated anti-CD45 antibodies, and subjected

to negative selection of CD45⁻ TSCs (*e.g.*, TECs and thymic fibroblasts) with MACS separation technology (Miltenyi Biotec, Auburn, CA). Approximately 0.25–0.5 million stromal cells were routinely obtained per thymus.

Lin⁻ progenitors were enriched from BM cells of 2–3-week-old B6.CD45.1 congenic mice (unless specified otherwise) with mouse Lineage cell depletion kit (Miltenyi Biotec), following the manufacturer's instructions. Lin⁻ progenitors and TSCs were mixed at 1 : 1 ratio and resuspended in RPMI-10 solution at a concentration of 5×10^7/ml. A 10 µl of cell mix (~0.5×10^6 cells) was injected into the decellularized thymus scaffolds using syringes with 32-G needles or pulled glass needles under the dissection scope. The reconstructed thymus organoids were cultured in the top chamber of a 3.5-cm transwell in RPMI-10 medium before being transplanted underneath the kidney capsules of 10–16-week-old B6.nude mice.

To evaluate T-cell development in the reconstructed thymus organoids, BM progenitors harvested from the B6 mice were mixed with TSCs isolated from C57BL/6.CD45.1 thymi at 1 : 1 ratio. The reconstructed thymus organoids were cultured in the upper chambers of 24-well transwell plates (one thymus per well; Corning, Tewksbury, MA) in complete RPMI-10 medium supplemented with 2 ng/ml interleukin-7 (Miltenyi Biotec) for 9 days. At the end of the culture, the thymus organoids were digested with Dispase I (0.6 U/ml, Roche Diagnostic, Indianapolis, IN) for 15 minutes at 37 °C. The isolated cells were stained with anti-CD45.2, anti-CD3, anti-CD4, and anti-CD8 antibodies for FCM analysis.

Stimulation of peripheral T-cells. T-cells isolated from the spleens and/or lymph nodes of Tot.B6.nude mice were labeled with CFSE and were subjected to stimulation with either anti-CD3 antibodies or allogeneic cells isolated from the spleens of CBA/J or Balb/C mice. Proliferation of T-cells under different stimulatory conditions was evaluated by the dilution of the intensities of CFSE signals with FCM analyses, as described earlier.[68,69] In brief, stock CFSE (5 mmol/l) was diluted at 1 : 1 ratio in HBSS. T-cells were resuspended at a concentration of 10×10^6 cells/ml, mixed with equal volumes of diluted CFSE, and incubated at 37 °C for 10 minutes. For assays with anti-CD3 antibody mediated stimulation, 5×10^5 of CFSE-labeled cells in 100 µl were added to wells of 96-well plates precoated with anti-CD3 (clone 500A2) antibodies and incubated for 72 hours. Cells were labeled with anti-CD4 and -CD8 antibodies, followed by staining with LIVE/DEAD Fixable Violet dead cell staining reagent for FCM analyses. For assays with allogeneic APCs as stimulants, 2.5×10^5 of CFSE-labeled cells in 100 µl were mixed with 2.5×10^5 T-cell depleted, mitomycin C (Sigma)-treated splenocytes harvested from CBA/J mice, added to wells of 96-well plates, and cultured for 4–7 days. Cells were labeled as described earlier for FCM analyses. In addition, cells were stained with anti-H2-K^k and anti-H2-K^b antibodies to label the stimulator (CBA/J) and responder (Tot.B6.nude) populations, respectively. Unless specified otherwise, all the experiments were run in triplicate and repeated at least three times.

Histology and immunohistochemistry. Reconstructed thymus organoids and kidneys were fixed in 4% paraformaldehyde for 3 hours at 4 °C and placed in 30% sucrose overnight. Cryosections of 7 µm thick were cut and stained with primary antibodies. Antibodies used in the study: Epcam (g8.8), B220, CD45, CD4, and CD8 (BD Biosciences, Franklin Lakes, NJ), rabbit antilaminin, rabbit anticollagen I, rabbit anticollagen IV, rabbit anti-fibronectin (Abcam, 1:200).

Detection of humoral responses against ovalbumin and peptides. Tot. B6.nude mice ($n = 5$) were immunized with subcutaneous injection of 50 µg of the OVA protein (Invivogen, San Diego, CA) emulsified in complete

Table 1 Sequences of primers for RT-PCR analysis of gene expression

Genes	Primers	Annealing temperature (°C)	Number of cycles	PCR size (base pairs)
Ins2	F 5′-CGC CGT GAA GTG GAG GAC-3′	62	40	115
	R 5′-TCTACAATGCCACGCTTCTG-3′			
Ica1	F 5′-TGAGTCTGCAACCTTCAACAGGGA-3′	58	42	141
	R 5′-AAACAGGGCCTTGACCCTCTCATT-3′			
Aire	F 5′-AATCTCCGCTGCAAATCCTGCTCT-3′	60	45	199
	R 5′-ACTGCAGGATGCCGTCAAATGAGT-3′			
Foxn1	F 5′-TGACGGAGCACTTCCCTTAC-3′	60	42	296
	R 5′-GACAGGTTATGGCGAACAGAA-3′			
CCL25	F 5′-GAGTGCCACCCTAGGTCATC-3′	60	40	87
	R 5′-CCAGCTGGTGCTTACTCTGA-3′			
Tbata	F 5′-TGACTCAGCCCACATTCTTATC-3′	58	40	353
	R 5′-GGGAACCCTTCTTGGATTTCT-3′			
Trp63	F 5′-GCTCATCATGCCTGGACTATTT-3′	60	42	352
	R 5′-CGCTCATTCTCCTTCCTCTTTG -3′			
EpCAM	F 5′-AGAATACTGTCATTTGCTCCAAACT-3′	58	40	110
	R 5′-GTTCTGGATCGCCCCTTC-3′			
Krt5	F 5′-CAGGGCACCAAGACCATAAA-3′	58	40	332
	R 5′-CTGTTGCAGCTCCTCATACTT-3′			
Krt8	F 5′-CGTCTGTGGTGCTGTCTATG-3′	58	40	332
	R 5′-CTTGGTCTGGGCATCCTTAAT-3′			
18S	F 5'-AAACGGCTACCACATCCAAG-3'	60	28	113
	R 5'-CCTCCAATGGATCCTCGTTA-3'			

Freund's adjuvant at the tail bases, followed by intraperitoneal injection of 25 μg of OVA in incomplete Freund's adjuvant to boost the immune responses 1 week later. Wild-type B6 mice ($n = 5$), as well as B6.nude mice transplanted with empty thymic scaffolds ($n = 3$), were also immunized similarly, as positive and negative controls, respectively.

Sera were harvested 6 weeks postimmunization, and the presence of anti-OVA Ig was examined with the mouse monoclonal antibody isotyping reagents kit (Sigma-Aldrich), following manufacturer suggested protocol. In brief, wells of 96-well ELISA plate were coated with 1 μg of OVA in 100 μl of PBS for 2 hours at 37 °C and incubated with 100 μl of diluted sera samples (1 : 50 dilution) overnight at 4 °C. Monoclonal antibody specific to different Ig isotypes (1 : 1000 dilution) was added to each of the wells and incubated for 2 hours at room temperature. After wash, 100 μl of the peroxidase labeled goat antimouse IgG antibody (1 : 5000) was added to each well and incubated at room temperature for 30 minutes. After wash, TMB substrate (BioLegned, San Diego, CA) was added to each well and the absorbance was measured at 450 nm (–570 nm for wavelength correction) with microplate reader (Molecular Devices, Sunnyvale, CA). The experiments were run in triplicate and repeated three times.

ELISPot analysis. ELISPot was performed using the BD mouse IFN-γ set (BD Biosciences), as described earlier.[70] In brief, splenocytes were isolated from OVA peptide immunized Tot.B6.nude ($n = 4$), or B6 controls ($n = 4$), suspended at 4.5×10^6/ml concentration in RMPI-10 and cultured for 24 hours at 37 °C, in the presence of 50 μg/ml OVA peptides (AVHAAHAEINEAGSIINFEKL). Unattached cells were harvested, washed, counted, and resuspended at 3×10^6 cells/ml in RPMI-10, supplemented with 50 μg/ml OVA peptides. 1×10^6 cells were seeded to one well of 96-well ELISPot plate (MSIPS4W 10, EMD Millipore, Thermo Fisher Scientific, Waltham, MA), precoated with 0.5 μg of anti-IFNγ capture antibody (BD Biosciences), and cultured overnight at 37 °C. At least 3×10^6 cells (10 wells) were analyzed for each sample. The wells were subsequently stained with horseradish peroxidase-conjugated, detection antibodies. IFN-γ-producing cells were visualized with AEC substrate set (BD Biosciences) and analyzed with CTL-ImmunoSpot S6 Micro Analyzer (Cellular Technology, Ltd., Shaker Heights, OH). The assays were repeated at least three times.

Detection of live cells in the reconstructed thymus organoids. Live cells in the thymus organoids cultured *in vitro* were detected with LIVE/DEAD viability kit for mammalian cells (Lifetechnologies, Grand Island, NY), following the fluorescence microscopy protocol suggested by the manufacturer. The kit discriminates live from dead cells by simultaneously staining with green-fluorescent calcein-AM, an indicator of intracellular esterase activity, and red-fluorescent ethidium homodimer-1, an indicator of loss of plasma membrane integrity. In brief, reconstructed thymus organoids were washed extensively with Dulbecco's phosphate-buffered saline (D-PBS). Staining solution was prepared by diluting stock solutions of both ethidium homodimer-1 and calcein-AM in D-PBS to a final concentration of 4 and 2 μmol/l, respectively. The thymus organoids were incubated in the staining solution for 30 minutes at room temperature and examined under the inverted laser scanning fluorescence microscope (FV1000, Olympus, Center Valley, PA).

In some experiments, TSCs were labeled with CFSE before being injected into the acellular thymus scaffolds. The presence and distribution of $CFSE^+$ cells in the reconstructed thymus organoids cultured *in vitro* were followed under the fluorescence microscope for up to 4 weeks.

RNA analysis. Total RNA was extracted from 250,000 TSCs and reconstructed thymus organoids cultured *in vitro* with RNeasy micro kit, according to the manufacturer's protocol (Qiagen, Valencia, CA). Following DNase I treatment (Ambion), RNA samples were reverse-transcribed into cDNAs with Superscript III cDNA kit, with random hexamers as primers for the RT reaction (Invitrogen). Semiquantitative PCR was performed as described earlier.[71] cDNA samples were diluted serially (1 : 5), and equal volumes of dilutents were used as templates for PCR amplification of the gene of interest. Sequences of primer pairs and conditions are listed in **Table 1** as in what follows.

FCM. The FCM analysis was performed on the BD FACSCalibur flow cytometer (BD Biosciences, San Jose, CA) and analyzed with either the CellQuest Pro software (BD Biosciences) or Flowjo. Single cell suspensions were prepared from spleen, subjected to erythrocyte depletion in red blood cell lysis buffer (Sigma-Aldrich), blocked with anti-CD16/32 antibody, and then stained with the other antibodies. The following antibodies were purchased from BD Biosciences: anti-CD16/32 (2.4G2), anti-CD4 (H129.9), anti-CD45 (30-F11), anti-CD3 (145-2C11), anti-CD45.1 (A20), anti-CD45.2 (104), anti-Epcam (g8.8), anti-CD62L (MEL-14), anti-CD69 (H1.2F3), and anti-CD44 (IM7). Anti-CD25 (7D4) antibody was purchased from Miltenyi Biotec. Staining buffer: PBS (calcium and magnesium free, Invitrogen) supplemented with 1% bovine serum albumin (Sigma-Aldrich) and 0.1% sodium azide (Sigma-Aldrich). Intracellular staining of the Foxp3 and Helios protein was performed with commercial kit purchased from eBiosciences (San Diego, CA), following manufacturer's suggested protocol.

SEM. Native and decellularized thymi were fixed in 2.5% glutaraldehyde in 0.1 M PBS (pH 7.4) for 60 minutes. The samples were washed thoroughly in 0.1 M PBS three times for 15 minutes each. Next, the samples were fixed in 1% osmium tetroxide in 0.1 M PBS for 60 minutes. This was followed by another three rounds of PBS washing steps for 15 minutes each. The samples were then dehydrated in gradient series of alcohol for 15 minutes each. In addition, samples were critical point dried and coated with Au/Pd using a Cressington Coater 108A sputter coater. Electron microscope images were taken using a Jeol JSM-6335F field emission SEM.

Statistical analysis. All values are expressed as the mean ± SEM unless otherwise specified. In mouse studies, statistical significance was determined using nonparametric Mann–Whitney test. All statistical analyses were carried out with the GraphPad Prism 4.0 Software. In all experiments, differences were considered significant when $P < 0.05$.

SUPPLEMENTARY MATERIAL

Figure S1. Reconstruction of thymus organoids with decellularized 3-D thymus scaffolds.
Figure S2. Fluorescence microscopy images of reconstructed thymus organoids.
Figure S3. Frequencies of thymic epithelial progenitor cells (TEPCs) in reconstructed thymus organoids cultured *in vitro*.
Figure S4. Reconstructed thymus organoids support T-cell development in vitro.
Figure S5. FCM analyses of the diverse distribution of T-cell receptor (TCR) Vβ genes.
Figure S6. Diversity of TCR Vβ genes in Tot.B6.nude mice determined by next-generation-sequencing-spectratyping (NGS-S).
Video S1. 3-D animation of the reconstructed thymus organoid.
Video S2. Representative 3-D composition of images of Epcam+ TECs in thymus organoids.
Video S3. Representative composite images of CD4+ and/or CD8+ T-cells in reconstructed thymus organoid.

ACKNOWLEDGMENTS

The authors thank Paul Dascani, Ann Piccirillo, Robert Lakomy, and Alex Styche for their exemplary technical assistance. The authors also thank Nick Giannoukakis for insightful discussions and suggestions. This study was supported by Department of Defense grant # W81XWH-09-1-0742 and the Henry Hillman Endowed Chair to M.T. The authors declare no competing financial interests.

REFERENCES

1. Fink, PJ (2013). The biology of recent thymic emigrants. *Annu Rev Immunol* **31**: 31–50.
2. Boehm, T (2008). Thymus development and function. *Curr Opin Immunol* **20**: 178–184.
3. Heng, TS, Chidgey, AP and Boyd, RL (2010). Getting back at nature: understanding thymic development and overcoming its atrophy. *Curr Opin Pharmacol* **10**: 425–433.
4. Fletcher, AL, Calder, A, Hince, MN, Boyd, RL and Chidgey, AP (2011). The contribution of thymic stromal abnormalities to autoimmune disease. *Crit Rev Immunol* **31**: 171–187.

5. Takada, K, Ohigashi, I, Kasai, M, Nakase, H and Takahama, Y (2014). Development and function of cortical thymic epithelial cells. *Curr Top Microbiol Immunol* **373**: 1–17.
6. Anderson, G and Takahama, Y (2012). Thymic epithelial cells: working class heroes for T cell development and repertoire selection. *Trends Immunol* **33**: 256–263.
7. Gill, J, Malin, M, Holländer, GA and Boyd, R (2002). Generation of a complete thymic microenvironment by MTS24(+) thymic epithelial cells. *Nat Immunol* **3**: 635–642.
8. Bennett, AR, Farley, A, Blair, NF, Gordon, J, Sharp, L and Blackburn, CC (2002). Identification and characterization of thymic epithelial progenitor cells. *Immunity* **16**: 803–814.
9. Nitta, T, Ohigashi, I, Nakagawa, Y and Takahama, Y (2011). Cytokine crosstalk for thymic medulla formation. *Curr Opin Immunol* **23**: 190–197.
10. Zartman, JJ and Shvartsman, SY (2010). Unit operations of tissue development: epithelial folding. *Annu Rev Chem Biomol Eng* **1**: 231–246.
11. van Ewijk, W, Wang, B, Hollander, G, Kawamoto, H, Spanopoulou, E, Itoi, M *et al.* (1999). Thymic microenvironments, 3-D versus 2-D? *Semin Immunol* **11**: 57–64.
12. Calderón, L and Boehm, T (2012). Synergistic, context-dependent, and hierarchical functions of epithelial components in thymic microenvironments. *Cell* **149**: 159–172.
13. Bonfanti, P, Claudinot, S, Amici, AW, Farley, A, Blackburn, CC and Barrandon, Y (2010). Microenvironmental reprogramming of thymic epithelial cells to skin multipotent stem cells. *Nature* **466**: 978–982.
14. Flomerfelt, FA, El Kassar, N, Gurunathan, C, Chua, KS, League, SC, Schmitz, S *et al.* (2010). Tbata modulates thymic stromal cell proliferation and thymus function. *J Exp Med* **207**: 2521–2532.
15. Marshall, D, Bagley, J, Le, P, Hogquist, K, Cyr, S, Von Schild, E *et al.* (2003). T cell generation including positive and negative selection ex vivo in a three-dimensional matrix. *J Hematother Stem Cell Res* **12**: 565–574.
16. Anderson, KL, Moore, NC, McLoughlin, DE, Jenkinson, EJ and Owen, JJ (1998). Studies on thymic epithelial cells *in vitro*. *Dev Comp Immunol* **22**: 367–377.
17. Pinto, S, Schmidt, K, Egle, S, Stark, HJ, Boukamp, P and Kyewski, B (2013). An organotypic coculture model supporting proliferation and differentiation of medullary thymic epithelial cells and promiscuous gene expression. *J Immunol* **190**: 1085–1093.
18. Chung, B, Montel-Hagen, A, Ge, S, Blumberg, G, Kim, K, Klein, S *et al.* (2014). Engineering the human thymic microenvironment to support thymopoiesis in vivo. *Stem Cells* **32**: 2386–2396.
19. Orlando, G, Soker, S and Stratta, RJ (2013). Organ bioengineering and regeneration as the new Holy Grail for organ transplantation. *Ann Surg* **258**: 221–232.
20. Gilbert, TW, Sellaro, TL and Badylak, SF (2006). Decellularization of tissues and organs. *Biomaterials* **27**: 3675–3683.
21. Ott, HC, Matthiesen, TS, Goh, SK, Black, LD, Kren, SM, Netoff, TI *et al.* (2008). Perfusion-decellularized matrix: using nature's platform to engineer a bioartificial heart. *Nat Med* **14**: 213–221.
22. Goh, SK, Bertera, S, Olsen, P, Candiello, JE, Halfter, W, Uechi, G *et al.* (2013). Perfusion-decellularized pancreas as a natural 3D scaffold for pancreatic tissue and whole organ engineering. *Biomaterials* **34**: 6760–6772.
23. Shin'oka, T, Imai, Y and Ikada, Y (2001). Transplantation of a tissue-engineered pulmonary artery. *N Engl J Med* **344**: 532–533.
24. Schechner, JS, Crane, SK, Wang, F, Szeglin, AM, Tellides, G, Lorber, MI *et al.* (2003). Engraftment of a vascularized human skin equivalent. *FASEB J* **17**: 2250–2256.
25. Sjöqvist, S, Jungebluth, P, Lim, ML, Haag, JC, Gustafsson, Y, Lemon, G *et al.* (2014). Experimental orthotopic transplantation of a tissue-engineered oesophagus in rats. *Nat Commun* **5**: 3562.
26. Ott, HC, Clippinger, B, Conrad, C, Schuetz, C, Pomerantseva, I, Ikonomou, L *et al.* (2010). Regeneration and orthotopic transplantation of a bioartificial lung. *Nat Med* **16**: 927–933.
27. Song, JJ, Guyette, JP, Gilpin, SE, Gonzalez, G, Vacanti, JP and Ott, HC (2013). Regeneration and experimental orthotopic transplantation of a bioengineered kidney. *Nat Med* **19**: 646–651.
28. Uygun, BE, Soto-Gutierrez, A, Yagi, H, Izamis, ML, Guzzardi, MA, Shulman, C *et al.* (2010). Organ reengineering through development of a transplantable recellularized liver graft using decellularized liver matrix. *Nat Med* **16**: 814–820.
29. Petersen, TH, Calle, EA, Zhao, L, Lee, EJ, Gui, L, Raredon, MB *et al.* (2010). Tissue-engineered lungs for *in vivo* implantation. *Science* **329**: 538–541.
30. Macchiarini, P, Jungebluth, P, Go, T, Asnaghi, MA, Rees, LE, Cogan, TA *et al.* (2008). Clinical transplantation of a tissue-engineered airway. *Lancet* **372**: 2023–2030.
31. Goh, SK, Olsen, P and Banerjee, I (2013). Extracellular matrix aggregates from differentiating embryoid bodies as a scaffold to support ESC proliferation and differentiation. *PLoS One* **8**: e61856.
32. Fan, Y, Rudert, WA, Grupillo, M, He, J, Sisino, G and Trucco, M (2009). Thymus-specific deletion of insulin induces autoimmune diabetes. *EMBO J* **28**: 2812–2824.
33. Bleul, CC, Corbeaux, T, Reuter, A, Fisch, P, Mönting, JS and Boehm, T (2006). Formation of a functional thymus initiated by a postnatal epithelial progenitor cell. *Nature* **441**: 992–996.
34. Corbeaux, T, Hess, I, Swann, JB, Kanzler, B, Haas-Assenbaum, A and Boehm, T (2010). Thymopoiesis in mice depends on a Foxn1-positive thymic epithelial cell lineage. *Proc Natl Acad Sci USA* **107**: 16613–16618.
35. Klein, L, Hinterberger, M, Wirnsberger, G and Kyewski, B (2009). Antigen presentation in the thymus for positive selection and central tolerance induction. *Nat Rev Immunol* **9**: 833–844.
36. Mathis, D and Benoist, C (2009). Aire. *Annu Rev Immunol* **27**: 287–312.
37. Bonner, SM, Pietropaolo, SL, Fan, Y, Chang, Y, Sethupathy, P, Morran, MP *et al.* (2012). Sequence variation in promoter of Ica1 gene, which encodes protein implicated in type 1 diabetes, causes transcription factor autoimmune regulator (AIRE) to increase its binding and down-regulate expression. *J Biol Chem* **287**: 17882–17893.
38. Depreter, MG, Blair, NF, Gaskell, TL, Nowell, CS, Davern, K, Pagliocca, A *et al.* (2008). Identification of Plet-1 as a specific marker of early thymic epithelial progenitor cells. *Proc Natl Acad Sci USA* **105**: 961–966.
39. Manley, NR, Richie, ER, Blackburn, CC, Condie, BG and Sage, J (2011). Structure and function of the thymic microenvironment. *Front Biosci (Landmark Ed)* **16**: 2461–2477.
40. Wong, K, Lister, NL, Barsanti, M, Lim, JM, Hammett, MV, Khong, DM *et al.* (2014). Multilineage potential and self-renewal define an epithelial progenitor cell population in the adult thymus. *Cell Rep* **8**: 1198–1209.
41. Foss, DL, Donskoy, E and Goldschneider, I (2001). The importation of hematogenous precursors by the thymus is a gated phenomenon in normal adult mice. *J Exp Med* **193**: 365–374.
42. De Barros, SC, Zimmermann, VS and Taylor, N (2013). Concise review: hematopoietic stem cell transplantation: targeting the thymus. *Stem Cells* **31**: 1245–1251.
43. Krell, PF, Reuther, S, Fischer, U, Keller, T, Weber, S, Gombert, M *et al.* (2013). Next-generation-sequencing-spectratyping reveals public T-cell receptor repertoires in pediatric very severe aplastic anemia and identifies a β chain CDR3 sequence associated with hepatitis-induced pathogenesis. *Haematologica* **98**: 1388–1396.
44. Min, B and Paul, WE (2005). Endogenous proliferation: burst-like CD4 T cell proliferation in lymphopenic settings. *Semin Immunol* **17**: 201–207.
45. Thornton, AM, Korty, PE, Tran, DQ, Wohlfert, EA, Murray, PE, Belkaid, Y *et al.* (2010). Expression of Helios, an Ikaros transcription factor family member, differentiates thymic-derived from peripherally induced Foxp3+ T regulatory cells. *J Immunol* **184**: 3433–3441.
46. Rae, M (2013). First Glimpse of Thymic Rejuvenation. Vol. 2013. http://sens.org/research/research-blog/first-glimpse-thymic-rejuvenation.
47. Falcon, J (2013). Techniques for thymic decellularization. *J Immunol* **190**: 135.28.
48. Komori, J, Boone, L, DeWard, A, Hoppo, T and Lagasse, E (2012). The mouse lymph node as an ectopic transplantation site for multiple tissues. *Nat Biotechnol* **30**: 976–983.
49. Posselt, AM, Barker, CF, Tomaszewski, JE, Markmann, JF, Choti, MA and Naji, A (1990). Induction of donor-specific unresponsiveness by intrathymic islet transplantation. *Science* **249**: 1293–1295.
50. Gottrand, G, Taleb, K, Ragon, I, Bergot, AS, Goldstein, JD and Marodon, G (2012). Intrathymic injection of lentiviral vector curtails the immune response in the periphery of normal mice. *J Gene Med* **14**: 90–99.
51. Wekerle, T and Sykes, M (2001). Mixed chimerism and transplantation tolerance. *Annu Rev Med* **52**: 353–370.
52. Chu, Q, Moreland, RJ, Gao, L, Taylor, KM, Meyers, E, Cheng, SH *et al.* (2010). Induction of immune tolerance to a therapeutic protein by intrathymic gene delivery. *Mol Ther* **18**: 2146–2154.
53. Poznansky, MC, Evans, RH, Foxall, RB, Olszak, IT, Piascik, AH, Hartman, KE *et al.* (2000). Efficient generation of human T cells from a tissue-engineered thymic organoid. *Nat Biotechnol* **18**: 729–734.
54. Seach, N, Mattesich, M, Abberton, K, Matsuda, K, Tilkorn, DJ, Rophael, J *et al.* (2010). Vascularized tissue engineering mouse chamber model supports thymopoiesis of ectopic thymus tissue grafts. *Tissue Eng Part C Methods* **16**: 543–551.
55. Alpdogan, O, Hubbard, VM, Smith, OM, Patel, N, Lu, S, Goldberg, GL *et al.* (2006). Keratinocyte growth factor (KGF) is required for postnatal thymic regeneration. *Blood* **107**: 2453–2460.
56. Erickson, M, Morkowski, S, Lehar, S, Gillard, G, Beers, C, Dooley, J *et al.* (2002). Regulation of thymic epithelium by keratinocyte growth factor. *Blood* **100**: 3269–3278.
57. Kermani, H, Goffinet, L, Mottet, M, Bodart, G, Morrhaye, G, Dardenne, O *et al.* (2012). Expression of the growth hormone/insulin-like growth factor axis during Balb/c thymus ontogeny and effects of growth hormone upon ex vivo T cell differentiation. *Neuroimmunomodulation* **19**: 137–147.
58. Dudakov, JA, Hanash, AM, Jenq, RR, Young, LF, Ghosh, A, Singer, NV *et al.* (2012). Interleukin-22 drives endogenous thymic regeneration in mice. *Science* **336**: 91–95.
59. Bredenkamp, N, Nowell, CS and Blackburn, CC (2014). Regeneration of the aged thymus by a single transcription factor. *Development* **141**: 1627–1637.
60. Jin, X, Nowell, CS, Ulyanchenko, S, Stenhouse, FH and Blackburn, CC (2014). Long-term persistence of functional thymic epithelial progenitor cells *in vivo* under conditions of low FOXN1 expression. *PLoS One* **9**: e114842.
61. Sun, X, Xu, J, Lu, H, Liu, W, Miao, Z, Sui, X *et al.* (2013). Directed differentiation of human embryonic stem cells into thymic epithelial progenitor-like cells reconstitutes the thymic microenvironment in vivo. *Cell Stem Cell* **13**: 230–236.
62. Parent, AV, Russ, HA, Khan, IS, LaFlam, TN, Metzger, TC, Anderson, MS *et al.* (2013). Generation of functional thymic epithelium from human embryonic stem cells that supports host T cell development. *Cell Stem Cell* **13**: 219–229.
63. Inami, Y, Yoshikai, T, Ito, S, Nishio, N, Suzuki, H, Sakurai, H *et al.* (2011). Differentiation of induced pluripotent stem cells to thymic epithelial cells by phenotype. *Immunol Cell Biol* **89**: 314–321.
64. Bredenkamp, N, Ulyanchenko, S, O'Neill, KE, Manley, NR, Vaidya, HJ and Blackburn, CC (2014). An organized and functional thymus generated from FOXN1-reprogrammed fibroblasts. *Nat Cell Biol* **16**: 902–908.
65. Hsu, PD, Lander, ES and Zhang, F (2014). Development and applications of CRISPR-Cas9 for genome engineering. *Cell* **157**: 1262–1278.
66. Mali, P, Yang, L, Esvelt, KM, Aach, J, Guell, M, DiCarlo, JE *et al.* (2013). RNA-guided human genome engineering via Cas9. *Science* **339**: 823–826.
67. Seach, N, Wong, K, Hammett, M, Boyd, RL and Chidgey, AP (2012). Purified enzymes improve isolation and characterization of the adult thymic epithelium. *J Immunol Methods* **385**: 23–34.
68. Quah, BJ and Parish, CR (2012). New and improved methods for measuring lymphocyte proliferation *in vitro* and *in vivo* using CFSE-like fluorescent dyes. *J Immunol Methods* **379**: 1–14.
69. Hogquist, KA (2001). Assays of thymic selection. Fetal thymus organ culture and *in vitro* thymocyte dulling assay. *Methods Mol Biol* **156**: 219–232.
70. Fan, Y, Gualtierotti, G, Tajima, A, Grupillo, M, Coppola, A, He, J *et al.* (2014). Compromised central tolerance of ICA69 induces multiple organ autoimmunity. *J Autoimmun* **53**: 10–25.
71. Fan, Y, Menon, RK, Cohen, P, Hwang, D, Clemens, T, DiGirolamo, DJ *et al.* (2009). Liver-specific deletion of the growth hormone receptor reveals essential role of growth hormone signaling in hepatic lipid metabolism. *J Biol Chem* **284**: 19937–19944.